

The multi-decadal hazard cascade of a tropical mountain wildfire

William Veness¹, Martha Day¹, Anthony C. Ross¹, Yazidhi Bamutaze², Jiayuan Han¹, Douglas Mulangwa^{3,4}, Andrew Mwesigwa⁴, Emmanuel Ntale⁵, Callist Tindimugaya⁴, Brian Guma⁴, Elisabeth Stephens^{3,6}, Wouter Buytaert¹

¹Department of Civil and Environmental Engineering, Imperial College London, London, SW7 2BB, UK

²Department of Geography, Geo-Informatics and Climatic Sciences, Makerere University, Kampala, Uganda

³Department of Meteorology, University of Reading, Reading, RG6 6BB, UK

⁴Ministry of Water and Environment, Kampala, Uganda

⁵Uganda Red Cross Society, Kampala, Uganda

⁶Red Cross Red Crescent Climate Centre, The Hague, The Netherlands

Correspondence to: William Veness (williamaveness@gmail.com)

Abstract. Climate change is driving wildfires to higher elevations, yet the hazard cascades that follow the burning of pristine tropical mountain ecosystems remain largely unexplored. Here, we analyse the long-term cascade following a February 2012 wildfire that burned 31 km² of forest and wetland in Uganda's Rwenzori Mountains National Park. Combining remote sensing, humanitarian records, field surveys, and interviews, we document ten major floods since 2012, including two debris floods that required large-scale humanitarian responses. Post-fire increases in erosion and mass movement have widened the River Nyamwamba sevenfold since 2012, breaching copper-cobalt mine tailings and mobilising an estimated 744,000 tonnes of waste into the river. Slow vegetation recovery at high altitudes and positive feedbacks between hazards have prolonged this high-risk state, underscoring the susceptibility of tropical mountain ecosystems to long-term post-wildfire cascades. More monitoring and research are required to characterise key hazard interactions after tropical mountain fires, which can guide entry points for management seeking to mitigate and ~~impede~~ future ~~easeades~~ hazards.

Style Definition: Normal

Style Definition: Heading 1

Style Definition: Heading 2

Style Definition: Heading 3

Style Definition: Heading 4

Style Definition: Hyperlink: Font color: Hyperlink

Style Definition: Betreff

Style Definition: Bullets

Style Definition: Header

Style Definition: Kontakt

Style Definition: Name

Style Definition: Copernicus_Word_template

Style Definition: MS title

Style Definition: List Paragraph

Style Definition: Affiliation

Style Definition: Equation

Style Definition: Footer

Style Definition: Correspondence

Style Definition: Bibliography

Formatted: Font color: Black

Formatted: Normal, Space Before: 9 pt, Border: Top: (No border), Bottom: (No border), Left: (No border), Right: (No border), Between : (No border)

Formatted: Font: 12 pt, Font color: Black

Formatted: Font color: Black

Formatted: Font color: Black

Formatted: Normal, Space Before: 6 pt, After: 18 pt, Border: Top: (No border), Bottom: (No border), Left: (No border), Right: (No border), Between : (No border)

Formatted: Font color: Black

Formatted: Normal, Border: Top: (No border), Bottom: (No border), Left: (No border), Right: (No border), Between : (No border), Tab stops: 7.96 cm, Centered + 15.92 cm, Right

1 Introduction

Climate and land-use changes are driving more frequent and intense wildfires across many tropical ecosystems worldwide (Ometto et al., 2022; UNEP, 2022; Wimberly et al., 2024; Obando-Cabrera et al., 2025). In tropical mountains, fires are burning at higher elevations (Xiao et al., 2022), which is exposing mature forests and wetlands that are not adapted to burning regimes. Tropical mountain forests cover 1.8 million km² globally (FAO & UNEP, 2020). ~~They~~, and they provide the headwaters of major river systems such as the Nile, Amazon and Mekong, ~~and~~ to sustain the livelihoods of over 336 million people (Encalada et al., 2019).

Hazard cascades describe networks of interconnected hazard processes, where a primary event initiates a sequence of subsequent hazards through direct or indirect interactions (Gill and Malamud, 2016). Understanding cascade dynamics is essential for risk assessment, as the cumulative impacts of cascading hazards often exceed those of individual events in isolation (Gill and Malamud, 2016). Tropical mountains host multiple hazards, making them susceptible to multi-hazard cascades (Arango-Carmona et al., 2025). Intense convectional rainfall drives flash floods; (Encalada et al., 2019), whilst high temperatures at lower elevations ~~cause~~ encourage the development of droughts, heatwaves and wildfires (Ometto et al., 2022); ~~and they are tectonically active (Sandwell et al., 2005). Their~~. In addition, their steep gradients, deeply chemically weathered soils, and unconsolidated glacial and fluvial deposits also favour landslides, debris flows and high rates of erosion (Arango-Carmona et al., 2025).

Multi-hazard cascades occur when two or more ~~of these~~ hazards interact through multiple relationships characterised as *triggering, probability increasing, or catalysing/impeding* (Gill and Malamud, 2016). Triggering interactions are typically short-term, through directly sequenced hazard events such as a lightning storm triggering a wildfire. Probability increasing interactions occur when a hazard affects the environmental conditions in a way that increases the likelihood of subsequent hazards occurring. Wildfires are known to have probability-increasing relationships with a range of secondary hazards due to the destruction of vegetation and changes to the physical, structural and biochemical properties of soil (Vahedifard et al., 2024; Boyer et al., 2022). For instance, the probability of post-fire flash flooding is increased due to vegetation-loss reducing interception and thus increasing effective precipitation (Stoof et al., 2012). Whilst triggering and probability increasing hazard interactions describe how one hazard affects the occurrence of another hazard, catalysis/impedance relationships act upon other hazard interaction pairings. For example, the increased river discharge resulting from wildfires may catalyse 'erosion-triggered-mass movements' by adding energy and material to earth flows, and the loss of vegetation in a wildfire-affected area may impede the development of future wildfires triggered by human activities (Shakesby and Doerr, 2006). In practice, hazards often share multiple of these cascading interactions, and their relationships can evolve over time (Gill and Malamud, 2016).

Formatted: Font color: Black

Formatted: Normal, Border: Top: (No border), Bottom: (No border), Left: (No border), Right: (No border), Between : (No border), Tab stops: 7.96 cm, Centered + 15.92 cm, Right

1.1 Post-Wildfire Hazard Cascades

Despite their increasing risk, wildfire hazard cascades in tropical montane regions remain poorly understood. Most existing research comes from temperate systems, where wildfires are known to amplify floods, accelerate erosion, and increase the probability of landslides and debris flows by removing vegetation, altering soil properties and increasing surface runoff (Belongia et al., 2023; Boyer et al., 2022; DeBano, 2000; Doerr et al., 2000; Guerriero et al., 2025; Jordan, 2016; Kemter et al., 2021; Rengers et al., 2020; Swain et al., 2025; Vahedifard et al., 2024); [McGuire et al., 2024](#)).

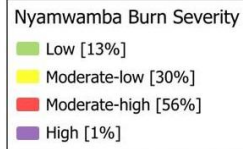
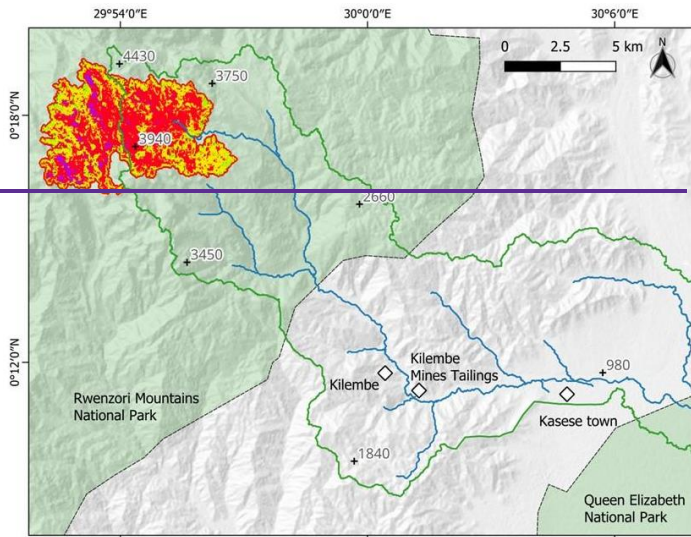
However, there are additional factors in tropical mountains that introduce [greater a unique](#) risk and complexity (Moazeni & Cerdà, 2024; Robinne et al., 2021). First, the fires impact upon an already diverse multi-hazard landscape with many existing hazard interactions (Arango-Carmona et al., 2025; Ometto et al., 2022; Sandwell et al., 2005). Second, many higher-altitude ecosystems within tropical mountains have no history of wildfire, such that mature climax vegetation and [pristine](#) wetlands are burned with unpredictable consequences for hydrological processes and ecosystem services (Marengo et al., 2021; Pivello et al., 2021; UNEP, 2022). Third, a lack of wildfire history means vulnerable populations without lived experience are exposed to new hazards (McCaffrey, 2004; Paton, 2003). Lastly, vegetation recovery at high altitudes is slow due to cold conditions, ~~a thinner atmosphere~~, and the presence of vegetation that is not adapted to fire cycles, causing prolonged impacts (Kappelle et al., 1996; Oliveras et al., 2014; Salinas et al., 2021). Given these differences, there is a need to better understand the long-term cascade of tropical montane wildfires at the process level. This is especially true for multi-hazard risk management, as identifying where hazards interact effectively highlights where those interactions can be proactively impeded (Aghakouchak et al., 2018, Aghakouchak et al., 2020; Vahedifard et al., 2024).

1.2 Rwenzori Mountains National Park 2012 Wildfire

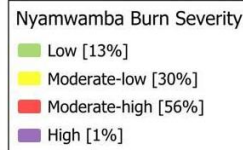
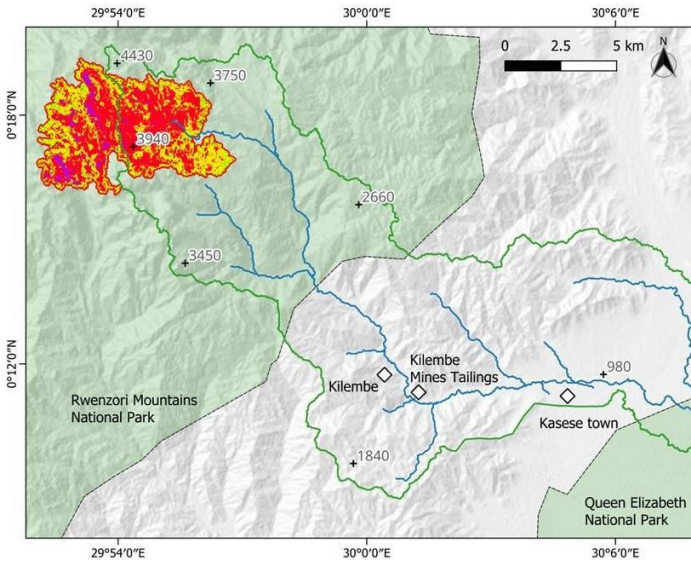
The February 2012 wildfire in Uganda's Rwenzori Mountains National Park burned 31 km² of pristine, uninhabited tropical mountain forest and wetlands (Fig. 1) during a brief meteorological drought measuring -3.5 in a 1-month Standardised Precipitation Index (Appendix A). The fire was followed by unprecedented debris flooding in May 2013 that displaced more than 25,000 people, caused 13 deaths and over USD \$4 million in damages (Delforge et al., 2025). Local rainfall records suggested only a 6.6-year return interval; [\(6-hour duration\)](#), indicating that post-fire landscape changes drove the disaster (Jacobs et al., 2016). ~~More~~[We present evidence that, more](#) than a decade later, the Nyamwamba catchment continues to experience flooding, debris ~~flows~~[floods](#), mass movements, erosion and water pollution ~~at elevated intensity due to fire-induced environmental changes~~. Because the wildfire occurred in a protected area with no burn history and little subsequent intervention (Norville, 2024), it provides an unparalleled case for this study to characterise the long-term multi-hazard cascade of a tropical mountain wildfire.

Formatted: Font color: Black

Formatted: Normal, Border: Top: (No border), Bottom: (No border), Left: (No border), Right: (No border), Between : (No border), Tab stops: 7.96 cm, Centered + 15.92 cm, Right



93



94

Formatted: Font color: Black
Formatted: Normal, Border: Top: (No border), Bottom: (No border), Left: (No border), Right: (No border), Between : (No border), Tab stops: 7.96 cm, Centered + 15.92 cm, Right

95 **Figure 4-1: The River Nyamwamba catchment and the delineated wildfire burn area within the Rwenzori Mountains, Uganda.**
96 **Differenced Normalised Burn Ratio (dNBR) between pre- and post-fire Landsat-7 images were used to delineate the extent and burn**
97 **severity of the February 2012 wildfire. Severity is classified according to the United States Geological Survey's guide (Key & Benson,**
98 **2006).**

99 1.3 The Study Region

100 The Rwenzori Mountains are an uplifted metamorphic basement block, with hard, crystalline basement geology creating steep
101 gradients and river profiles that climb to a maximum elevation of 5,109 m (UNESCO, 2012). It is the third largest glaciated
102 region in Africa (Hinzmann et al., 2024), with abundant quaternary deposits of unconsolidated glacial and fluvial sediment in
103 its valleys (UNESCO, 2012; Ring, 2008). The Rwenzori Mountains National Park is a UNESCO World Heritage Site dedicated
104 to the protection of biodiverse and unique montane flora, classified into five distinct eco-zones (UNESCO, 2012): tropical
105 mixed broadleaf montane rainforest (<2600 m altitude); bamboo forest (2600-3000 m); an ericaceous zone characterised by
106 dense giant heather trees, giant senecios and giant Lobelia (3000-3800 m); afro-alpine moorland and bogs (3800 – 4400 m);
107 and the rock, snowfield and glacier zone (>4400 m).

108
109 Higher altitudes within the equatorial mountain range have an annual precipitation of 2500 mm, with two wet seasons (March-
110 May and September-December) where monthly precipitation values exceed 375 mm (UNESCO, 2012). The River
111 Nyamwamba is a major river in the southern part of the Rwenzori Mountains that transports water to its delta with Lake George
112 within the Queen Elizabeth National Park area (Fig. 1).

113 1.4 Study Scope

114 This study characterizes the multi-decadal hazard cascade profile of the Nyamwamba River catchment following a 2012
115 wildfire that burned 31 km² of pristine tropical mountain forest and wetland in Uganda's Rwenzori Mountains National Park
116 and interprets the implications for regional risk management and broader lessons for tropical montane environments globally.
117 Through an integrated mixed-methods approach combining remote sensing analysis, humanitarian records, field surveys, and
118 semi-structured interviews, we document the long-term interactions between wildfire, flooding, erosion, landslides, and
119 pollution over a 12-year period (2012-2024). The study identifies key hazard interactions using Gill and Malamud's (2016)
120 framework, evaluates entry points for management interventions to mitigate future hazards in fire-sensitive tropical mountain
121 ecosystems, and derives take-aways for the governance and resilience of tropical montane regions facing emerging fire-driven
122 risks.

Formatted: Font: 9 pt, Bold, Font color: Black

Formatted: Font: 9 pt, Bold, Font color: Black

Formatted: Normal, Space After: 10 pt, Border: Top: (No border), Bottom: (No border), Left: (No border), Right: (No border), Between : (No border)

Formatted: Font color: Black

Formatted: Normal, Border: Top: (No border), Bottom: (No border), Left: (No border), Right: (No border), Between : (No border), Tab stops: 7.96 cm, Centered + 15.92 cm, Right

123 **2 Methods**

124 We adopted a mixed methods approach to evidence changes in multi-hazard processes and risk, combining remote sensing,
125 humanitarian data, field observations and key informant interviews. Cross-validation across methods enabled an abductive
126 approach (Saunders et al., 2016), where emerging insights, such as interview reports of erosion, informed subsequent lines of
127 data collection and analysis.

128 **2.1 Remote Sensing and GIS**

129 **2.1.1 Data Acquisition and Pre-Processing**

130 Annual Landsat-7 (2006 – 2012) and Landsat-8 (2013-2024) Level-2 surface reflectance images [at 30m resolution](#) were
131 downloaded from the United States Geological Survey (USGS) earth explorer and gap corrected, cropped and cloud masked
132 for analysis (Congedo, 2021). For each year, the earliest post-January 1 image with <10% cloud cover was selected. High-
133 resolution Google Earth Pro imagery was used to measure river width, while Maxar mosaics visualised mine tailings erosion
134 (Maxar Technologies, 2025a; Maxar Technologies, 2025b).

135 **2.1.2 Burn Severity Classification**

136 Burned area was delineated using the Normalised Burn Ratio (NBR), which combines Landsat 7 near-infrared (Band 4) and
137 shortwave-infrared (Band 7) reflectance (Key & Benson, 2006)-) [to map and quantify the severity of a fire's impact on](#)
138 [vegetation and soil](#). The difference between pre- (9 January 2012) and post-fire (28 March 2012) NBR values (dNBR) provided
139 a relative severity index following USGS protocols (Key & Benson, 2006).

140 **2.1.3 River [Channel Bank](#) Erosion Analysis**

141 Supervised minimum-distance land-cover classifications were applied to annual Landsat images from 2006 – 2024, using fixed
142 ground control points for five classes: eroded river channel, tailings, oxidised iron, vegetation, and agriculture (Congedo,
143 2021). Each image was clipped to the Nyamwamba channel, and classified areas were validated against Google Earth area
144 estimates with a relative error of 3.84%. Cumulative [lateral riverbank](#) eroded area was plotted over time, with classification
145 maps from 2006 and 2021 shown for comparison. River width was delineated in 2010, 2014, 2018, and 2021, at 1 km intervals
146 along 20 km of channel between Kilembe town and Lake George.

147 **2.1.4 Tailings Erosion**

148 Erosion of the Kilembe Mines tailings was assessed using Maxar mosaics from March 2006 and April 2023, with the 33,000
149 m² eroded footprint delineated manually. Field measurements in July 2024 using a laser rangefinder provided site dimensions,
150 from which eroded volumes were calculated (see Appendix B).

Formatted: Font color: Black

Formatted: Normal, Border: Top: (No border), Bottom: (No border), Left: (No border), Right: (No border), Between : (No border), Tab stops: 7.96 cm, Centered + 15.92 cm, Right

151 **2.2 Humanitarian Data Analysis**

152 Historic flood events in the Nyamwamba catchment since 2000 were compiled from multiple open sources: the Emergency
153 Events Database (Delforge et al., 2025), the Sendai DesInventar database (DesInventar, 2025), grey literature in ReliefWeb,
154 and a systematic keyword search (“Kasese” OR “Kilembe” AND “flood”) across Google, Google Scholar, and Google News
155 (Google News, 2025). While recent years benefit from expanded monitoring and reporting, the inclusion of diverse sources
156 provided confidence that all major flood events since 2000 were captured by the search.

157 **2.3 Interviews**

158 We conducted twelve in-person semi-structured interviews during field visits in 2023 and 2024, following ethical clearance.
159 Participants were identified through project partners in Kasese District, with snowball sampling to access other stakeholder
160 groups. They included 2 representatives from the Ministry of Water [M – code used to reference in the results], 2 local
161 government officials [G], 1 wildlife authority employee [W], 1 non-governmental organisation worker [N], 2 local industry
162 workers [I], 1 farmer [F], and 3 community residents [R].

163
164 Interviews followed a lightly structured topic guide covering hazard processes and causes, changing risk, existing management,
165 and potential alternatives, while remaining flexible to emergent themes (Creswell, 2009; Galletta, 2013; Mojtahed et al., 2014).
166 A full guide is provided in Appendix C. Interviews lasted 30 – 120 minutes, were audio-recorded, transcribed, and coded
167 inductively over two rounds of review, with related codes grouped into interpretive themes (Patton, 2014; Saldana, 2021).
168 While themes are not presented directly, this analysis informed interpretation of hazard processes, impacts, and management
169 options.

170 **2.4 Photographs**

171 Historic photographs of the vegetation pre- and immediately post-wildfire were taken by project partners with permission for
172 research use. Photographs in Appendices E – J were taken by the study authors during a July 2024 site visit.

173 **2.5 Cascade Visualisation**

174 Processes identified through the above methods were integrated into a conceptual diagram of the wildfire’s multi-hazard
175 cascade (Patton, 2014), following Gill & Malamud’s (2016) framework for hazard interaction types. Evidence underlying each
176 connection is documented throughout the Results and summarised in Table D1 (Appendix D).

177

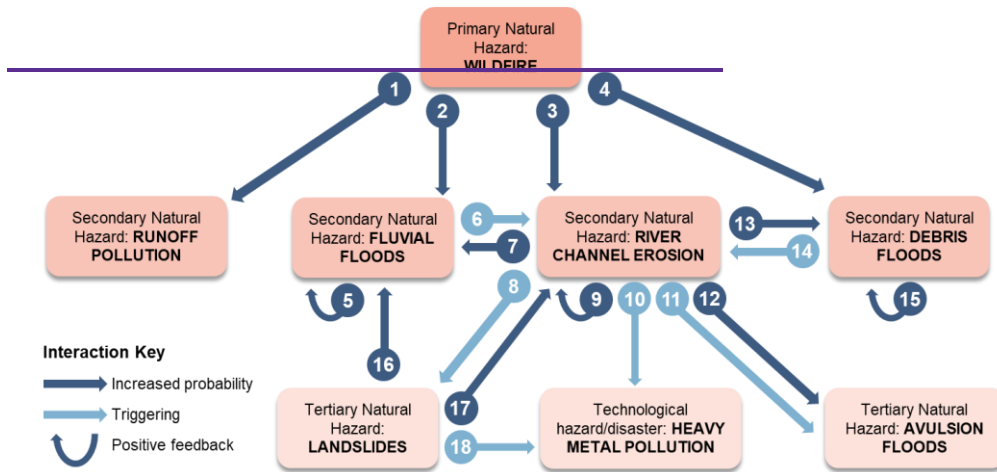
Formatted: Font color: Black

Formatted: Normal, Border: Top: (No border), Bottom: (No border), Left: (No border), Right: (No border), Between : (No border), Tab stops: 7.96 cm, Centered + 15.92 cm, Right

178 **3 Results**

179 We present the multi-hazard cascade caused by the 2012 Rwenzori National Park wildfire (Fig. 2). The following sections
180 describe each of the hazards involved and the interactions they drive, based on evidence from our mixed methods. Results are
181 structured by hazard type: wildfire (Sect. 3.1), flooding (3.2), landslides (3.3), erosion (3.4), and pollution (3.5). Identified
182 interactions highlight opportunities where management interventions can impede the cascade, for which we discuss practical
183 solutions at the local and global scales in Sect. 4 (Discussion). The hazard definitions follow the Hazard Information Profiles
184 (UNDRR, 2025) and are clarified in Table D1 (Appendix D). Importantly, here landslides refer to gravitational mass
185 movements directly connected to the river system as shown in Figures I1 and I2 (Appendix I).

186
187



188
189
190

Formatted: Font color: Black
Formatted: Normal, Border: Top: (No border), Bottom: (No border), Left: (No border), Right: (No border), Between : (No border), Tab stops: 7.96 cm, Centered + 15.92 cm, Right

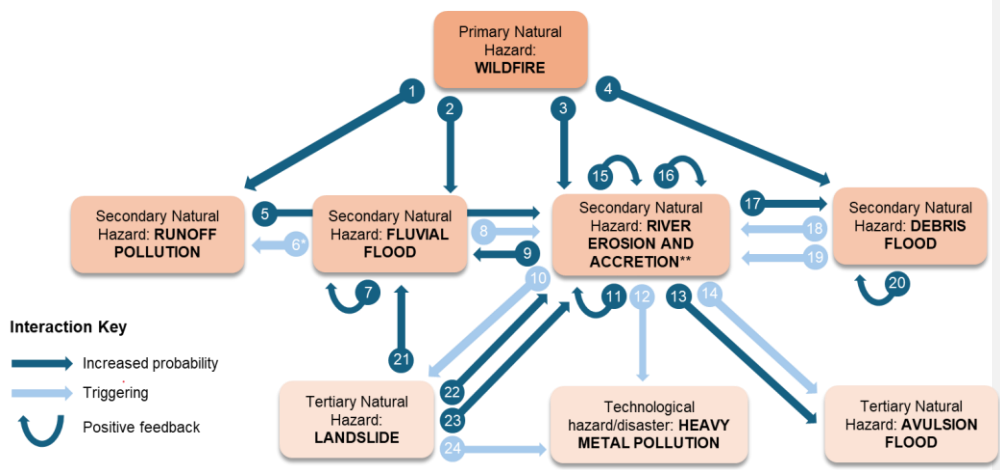


Figure 2: Conceptual model of the multi-hazard cascade following the Rwenzori National Park wildfire in February 2012. Interactions between hazards are classified as being (i) triggering, or (ii) probability increasing or (iii) catalysing/impeding, following Gill and Malamud's (2016) framework. As there, and (iii) positive feedbacks have been identified. There are numerous catalysing/impeding relationships in this context, which we omit these from the visualisation for simplicity but describe key examples in the analysis text. Table 1 describes each of the interactions shown.

*Interaction (6) also applies for debris floods and avulsion floods as the driving hazard (Table 1), but they are grouped for simplicity in the visualisation.

**River channel erosion and accretion of eroded sediment are treated as one hazard in line with UNDRR's Hazard Information Profiles (HIPs), with continuously interacting processes and positive feedbacks (15, 16) along the river's reach (UNDRR, 2025).

Table 1: Description of the hazard cascade interactions in Fig. 2. The study evidence for each interaction is explained in the text and summarised in Table D+D2 (Appendix D).

Driving Hazard	Description of Interaction	Affected Hazard
Wildfire	1 1	Runoff Pollution
	2 2	Fluvial Floods

9

9

Formatted: Font: 9 pt, Bold, Font color: Black

Formatted: Normal, Space After: 10 pt, Border: Top: (No border), Bottom: (No border), Left: (No border), Right: (No border), Between : (No border)

Formatted: Font: 9 pt, Bold, Font color: Black

Formatted: Font: 9 pt, Bold, Font color: Black

Formatted: Font: 9 pt, Bold, Font color: Black

Formatted: Font: 9 pt, Bold, Font color: Black

Formatted: Font: 9 pt, Bold, Font color: Black

Formatted: Font: 9 pt, Bold, Font color: Black

Formatted: Font: 9 pt, Bold, Font color: Black

Formatted: Font: 9 pt, Bold, Font color: Black

Formatted: Normal, Space After: 10 pt, Border: Top: (No border), Bottom: (No border), Left: (No border), Right: (No border), Between : (No border)

Formatted: Font: 9 pt, Bold, Font color: Black

Formatted: Font color: Black

Formatted: Normal, Border: Top: (No border), Bottom: (No border), Left: (No border), Right: (No border), Between : (No border), Tab stops: 7.96 cm, Centered + 15.92 cm, Right

	3	The higher peak river discharge has increased the river's erosive power	River-Erosion and Accretion
	4	The higher peak river discharge has increased its transport competence	Debris Floods
Runoff Pollution	5	<u>Increased sediment loads, more material available for accretion</u>	Erosion and Accretion
Fluvial Floods	6	<u>Floodwaters (fluvial, *avulsion and debris floods) transport contaminants across the landscape</u>	Runoff Pollution
Fluvial Floods	7	Each flood damages natural banks & flood defences	Fluvial Floods
	8	Higher flow velocities & turbulence during floods increase erosion	River-Channel-Erosion and Accretion
River Channel Erosion and Accretion	9	Eroded material fills the channel, reducing its discharge capacity	Fluvial Floods
	10	Lateral erosion undercuts & destabilises hillslopes	Landslides
	11	Lateral erosion exposes bare <u>river-cliffs/riverbanks</u> to further erosion	River-Channel-Erosion and Accretion
	12	Direct erosion inputs Co-Cu Kilembe Mines solid tailings into the river	Heavy Metal Pollution
	13	Higher erosion rates have increased channel-switching events	Avulsion Floods
	14	Eroded sediment deposits in channel bars, diverting flow to banks	Avulsion Floods
	15	<u>Sediment deposition narrows channel increasing erosive potential</u>	Erosion and Accretion
	16	<u>Eroded sediment accretes in the channel, diverting flow to erode riverbanks</u>	Erosion and Accretion
	17	Erosion generates additional sediment for debris <u>flow/flood</u> formation	Debris Floods
Debris Floods	18	<u>Debris floods have a high erosive power</u>	Erosion and Accretion
	19	<u>Mobilized sediment deposits in channel, diverting flow to erode riverbanks</u>	Erosion and Accretion
Debris Floods	20	Debris floods damage natural banks & flood defences	Debris Floods
	21	<u>Debris flows have a high erosive power</u>	River-Channel-Erosion
Landslides	22	Landslide talus fills the channel, reducing its discharge capacity	Fluvial Floods
	23	<u>Increased sediment loads, more material available for accretion</u>	Erosion and Accretion
	24	Landslides increase sediment loads, increasing erosion by abrasion	River-Channel-Erosion and Accretion

Merged Cells

Formatted: Font: Times New Roman, 10 pt, Not Bold

Split Cells

Formatted: Line spacing: single, Widow/Orphan control, Border: Top: (No border), Bottom: (No border), Left: (No border), Right: (No border), Between : (No border)

Formatted: Font: Times New Roman, 10 pt, Not Bold

Formatted: Font color: Text 1

Formatted: Font color: Text 1

Formatted: Font color: Text 1

Formatted: Font color: Text 1

Formatted: Font color: Text 1

Merged Cells

Formatted: Line spacing: Multiple 1.15 li, No widow/orphan control, Border: Top: (No border), Bottom: (No border), Left: (No border), Right: (No border), Between : (No border)

Formatted: Font: Times New Roman, 10 pt, Not Bold

Split Cells

Formatted: Font color: Red

Formatted: Font: Times New Roman, 10 pt, Not Bold

Formatted: Font color: Black

Formatted: Normal, Border: Top: (No border), Bottom: (No border), Left: (No border), Right: (No border), Between : (No border), Tab stops: 7.96 cm, Centered + 15.92 cm, Right

18
24

Rotational slumping of tailings inputs waste to the river channel

Heavy Metal Pollution

Formatted: Font: Times New Roman, 10 pt, Not Bold

209

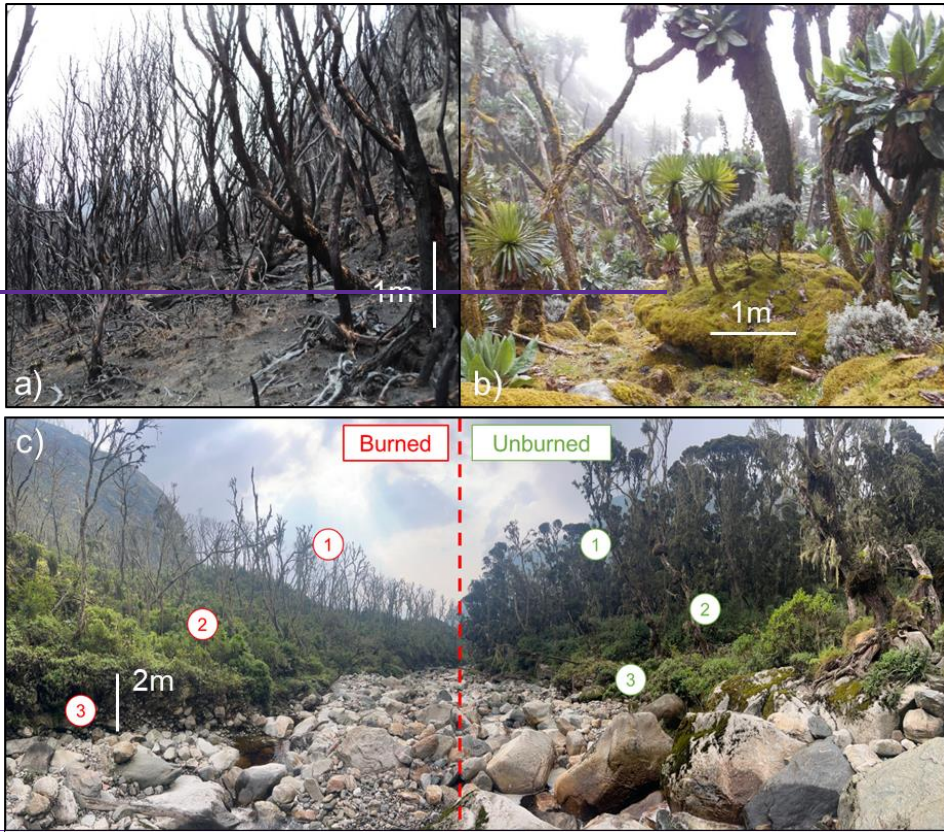
210 3.1 Wildfire

211 Remote sensing evidence shows a 30.75 km² burn area for the February 2012 wildfire (Fig. 1), with 87% of the area burned to
212 a moderate or high severity. The fire occurred during a meteorological drought, with <0.2 mm of precipitation in the 4-weeks
213 preceding the fire (Jacobs et al., 2016) and a one-month Standardised Precipitation Index measuring -3.5 for January 2012
214 (Appendix A). The ~~trigger~~fire's cause of the fire~~ignition~~ is still unknown by the water and wildlife authorities [M1; M2; W1].
215

216 The fire burned between 3360 – 4400 m above sea level, burning climax 'heather zone' forest, "spongy" [R1] Afroalpine
217 moorland, and methane-rich bogs [M1], all with no recorded history of wildfires. (Fig. 3a; UNEP, 2022). Photographs from
218 March 2012 show indicators of high burn severity (Fig. 3b), while images from July 2024, twelve years later, reveal regrowth
219 limited to a maximum of 2.5 m, with the upper canopy still vacant (Fig. 3c). These slow growth rates and an observed scarcity
220 of heather in the regrowth succession indicate that natural recovery will require several decades- ([Wesche, Miede and Kaeppli,
221 2000](#)).
222
223

Formatted: Font color: Black

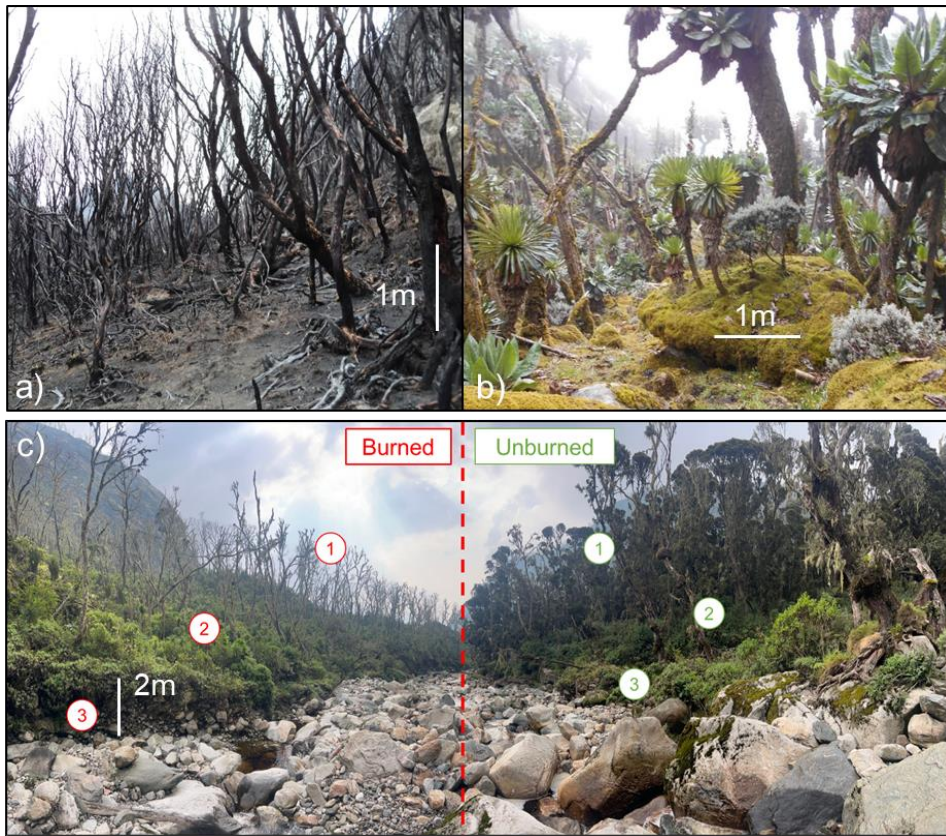
Formatted: Normal, Border: Top: (No border), Bottom: (No border), Left: (No border), Right: (No border), Between : (No border), Tab stops: 7.96 cm, Centered + 15.92 cm, Right



224

Formatted: Font color: Black

Formatted: Normal, Border: Top: (No border), Bottom: (No border), Left: (No border), Right: (No border), Between : (No border), Tab stops: 7.96 cm, Centered + 15.92 cm, Right



#	Attribute in c)	Burned	Unburned
1	Upper canopy	Dead ericaceous trees, vacant canopy	Mature ericaceous canopy
2	Lower canopy	Regrowth up to 2.5 m, heather scarce	Mature, dense vegetation
3	Riverbanks	Steep, unvegetated banks of exposed and unconsolidated glacial till	Sloped banks and coarse material anchored by vegetation

Figure 3: a) burned ericaceous 'heather zone' vegetation 1-month after the wildfire in March 2012; b) Mature Afroalpine moorland vegetation prior to the wildfire (March 2011); c) upper course of the River Nyamwamba at 3380 m elevation in July 2024, where the river had acted as a firebreak to provide direct comparison between unburned and recovering burned sections of the ericaceous forest. Scale bars correspond to the tree trunk in 3a, the boulder in 3b and the river-cliff/riverbank in 3c. The associated table describes the ecological properties of the burned and unburned areas.

Formatted: Font: 9 pt, Bold, Font color: Black

Formatted: Normal, Space After: 10 pt, Border: Top: (No border), Bottom: (No border), Left: (No border), Right: (No border), Between : (No border)

Formatted: Font: 9 pt, Bold, Font color: Black

Formatted: Font color: Black

Formatted: Normal, Border: Top: (No border), Bottom: (No border), Left: (No border), Right: (No border), Between : (No border), Tab stops: 7.96 cm, Centered + 15.92 cm, Right

232 *Wildfire-driven Interactions*

233 The wildfire has [unidirectional](#) probability-increasing ~~interaction~~[interactions](#) with four secondary hazards. First, burning of
234 soils and vegetation cover increased surface erosion and runoff to river channels, raising turbidity, carrying ash and peat, and
235 introducing biological contaminants. Respondents recalled a strong smell “like methane” after the fire [M1; M2; R1; G1],
236 highlighting wildfire-driven runoff pollution (#1). Second, reduced interception and infiltration capacity increased peak
237 discharges at shorter lag times, driving a marked rise in fluvial flooding (#2; Sect. 3.2). ~~Erosion~~[Riverbank erosion](#) has also
238 accelerated due to higher discharges and loss of root cohesion (#3; Sect. 3.4), which, together with higher peak flows after the
239 wildfire, enhanced the conditions for debris ~~flow~~[flood](#) formation due to greater sediment supply [M1; R1] (#4), [#17](#). [These](#)
240 [interactions \(#1 - 4\) are unidirectional because none of the secondary or tertiary hazards have resulted in further occurrence of](#)
241 [wildfires in the catchment.](#)

242
243 Additional relationships where the wildfire has catalysed other hazard interactions are numerous, but evidence for these cannot
244 fully be established without intensive monitoring and field experimentation. Based on hydrological theory, some interactions
245 catalysed by the wildfire’s effects would include:

- 247 • *River channel erosion-triggering-landslide (#810)*: increased discharge after the wildfire ([Moody and Martin, 2001](#))
248 catalyses the generation of landslides caused by erosive undercutting from higher river erosion rates ([Korup and](#)
249 [Schlunegger, 2007](#)).
- 251 • *Landslide-increasing probability-river erosion (#1223)*: increased discharge catalyses the contribution of landslides
252 to later erosion by transporting landslide talus and using the sediment as erosive tools for abrasion ([Sklar and](#)
253 [Dietrich, 2001](#)).
- 255 • *Debris flood-triggering-river erosion (#1418)*: increased discharge catalyses erosion during debris flood events by
256 increasing the erosive power of the ~~flow~~[flood](#) ([Stock and Dietrich, 2003](#)).
- 258 • *Landslide-increasing probability-fluvial flood (#1621)*: increased discharge increases the volume of water
259 accumulating in damming and bursting flood mechanisms after landslides ([Costa and Schuster, 1987; Rudoy, 2002](#)).

260
261 Although many of the other hazards in the cascade are responsible for additional catalysing relations, we only present examples
262 for the wildfire hazard in this study. This is to emphasise that the fire has not only increased the probability of four secondary
263 natural hazards at the start of the cascade, but it is also catalysing subsequent interactions between other hazards.

264

Formatted: Outline numbered + Level: 1 + Numbering Style:
Bullet + Aligned at: 0.63 cm + Indent at: 1.27 cm

Formatted: Outline numbered + Level: 1 + Numbering Style:
Bullet + Aligned at: 0.63 cm + Indent at: 1.27 cm

Formatted: Outline numbered + Level: 1 + Numbering Style:
Bullet + Aligned at: 0.63 cm + Indent at: 1.27 cm

Formatted: Outline numbered + Level: 1 + Numbering Style:
Bullet + Aligned at: 0.63 cm + Indent at: 1.27 cm

Formatted: Font color: Black

Formatted: Normal, Border: Top: (No border), Bottom: (No
border), Left: (No border), Right: (No border), Between : (No
border), Tab stops: 7.96 cm, Centered + 15.92 cm, Right

265 **3.2 Flooding**

266 All twelve respondents reported heightened flood risk in the Nyamwamba catchment. Five attributed this directly to changes
 267 in hydrological processes caused by the 2012 wildfire [M1; M2; G1; G2; R1], while others cited land use change [N1; W1;
 268 R3], climate change [N1; I2], or the discontinuation of dredging [I1; R2]. A government official explained that “*the burning*
 269 *is the reason we are now having the floods annually... we know how useful wetland vegetation is in controlling floods, releasing*
 270 *water slowly*” [G1]. Similarly, a local guide described the flood-buffering role of the alpine wetlands: “*the moss was like a big*
 271 *1 m thick sponge, it soaked up all the rain... 20 or 30 km² of rock that was once boulders covered in moss is now bare*” [R1].
 272 Table 2 documents ten flood events since 2012, all exceeding in intensity the two documented events during the preceding 12
 273 years, with the 2013 and 2020 debris floods requiring international humanitarian appeals (Act Alliance, 2020; Delforge et al.,
 274 2025; Okiror, 2020).

276 **Table 2: Timeline of flood events of the Nyamwamba River documented by humanitarian databases and grey literature since 2000.**
 277 **The dates of the two most intense debris flood events are highlighted bold.**

Date	Area(s) Affected	Description & Impacts
1 st May 2001	Rukoki, Kilembe	1 death and 300 people affected by flooding in Kasese District (Delforge et al., 2025; DesInventar, 2025)
8 th September 2010	Rukoki, Ihandiro	A house, truck, pipeline and fields of crops destroyed by minor riverine flooding (Delforge et al., 2025).
<i>February 2012 – Wildfire burns 30.75 km² of the Rwenzori National Park</i>		
1st & 5th May 2013	Kilembe, Kasese District	Flooding <u>and debris flooding</u> in the Nyamwamba, Mubuku, Bulemba and Kitakena rivers displaced 25,445, with 13 deaths and US\$4,055,000 of damage (Delforge et al., 2025). Formal humanitarian response appeal of \$220,497 made by ACT Alliance (Act Alliance, 2013).
14 th May 2014	Kasese town	3,725 affected and 4 deaths in Kasese (DesInventar, 2025).
18 th June 2014	Kilembe	Flooded hospital and secondary school (Asiimwe, 2014).
18 th April 2016	Kanamba, Kanaka, Kasese District	10,000 affected and an estimated \$3,428,000 of damage following flooding of the Nyamwamba, Sebwe and Mubuku rivers between 4 th – 18 th April (Delforge et al., 2025; DesInventar, 2025; Juma, 2016).
4 th July 2017	Kilembe	4 killed in the Kilembe Valley (DesInventar, 2025).
5th May 2020	Kasese District	173,000 people affected in 24,760 houses across Kasese and Bundibugyo Districts following flooding of major rivers (Delforge et al., 2025). <u>Debris and fluvial flooding on the River Nyamwamba-overflow</u> submerged the Kilembe Mines hospital, with over 1,200 people displaced in Kasese town (Act Alliance, 2020; Flood List News, 2020a, 2020b). Formal humanitarian appeal for assistance made by the Ugandan Red Cross to support the displaced (Okiror, 2020)
23 rd May 2021	Kilembe	3 deaths and 134 affected following flooding and landslides in Kilembe town (Delforge et al., 2025).

Formatted: Font: 9 pt, Bold, Font color: Black

Formatted: Normal, Space After: 10 pt, Border: Top: (No border), Bottom: (No border), Left: (No border), Right: (No border), Between: (No border)

Formatted: Font: 9 pt, Bold, Font color: Black

Formatted Table

Formatted: Font color: Black

Formatted: Normal, Border: Top: (No border), Bottom: (No border), Left: (No border), Right: (No border), Between: (No border), Tab stops: 7.96 cm, Centered + 15.92 cm, Right

18 th May 2023	Kasese District	1,016 people affected, and 23 deaths recorded between 24 th April and 18 th May due to multiple floods of the Muhokya, Mubuku, Sebwe and Nyamwamba rivers (Delforge et al., 2025).
22 nd May 2024	Kilembe, Kasese town	Sudden change of river course during high flow. Debris flows/floods , riverine flooding and mudslides in the Nyamwamba catchment displaced 5,389 people in Kasese town (New Vision, 2024).
7 th September 2024	Kasese Town	2 deaths and extensive damage to key infrastructure including schools, roads, bridges and 120 houses. Change of course of river during high flows breached same location as the 22 nd May 2024 flood (ReliefWeb, 2024).

The wildfire has increased the frequency and magnitude of fluvial flooding, but also introduced two new mechanisms of flooding, with gravity-driven debris floods and avulsion floods linked to increased mass movement (Sect. 3.3) and erosion (Sect. 3.4) in the catchment [M1; M2].

Fluvial flooding

Vegetation and soil loss following the wildfire reduced interception, infiltration, and water retention capacity, amplifying the river’s discharge response to rainfall. The fluvial flooding of unprecedented intensity on 5th May 2013 followed rainfall of only a 6.6-year estimated return period [for a 6-hour event](#) (Jacobs et al., 2016). Two respondents emphasise that a lack of lived experience prior to this first flood created additional vulnerability among affected communities: “2013 - that was when we were all surprised. I could not believe what I saw” [I1]; “we were not prepared because we had never experienced such magnitude” [M1]. Seven years later, an industrial worker recalled the 2020 event as “an 800 cumecs flood... higher than our professional hydrologist’s modelling of a 1000-year flood event” [I2].

Debris flooding

Two floods (2013 and 2020) included debris [flows/floods](#), confirmed in video footage and respondent testimony [M1; R1]. A water authority described “entire mahogany trees coming down as flood load” [M1], while a resident noted “moving rocks two times the size of a minibus” [R1]. Field photos (Appendix G) confirm extensive boulder deposition on the floodplain, and the river has since shifted from a pre-wildfire meandering form with vegetated banks to a braided morphology laden with coarse crystalline sediment (Appendix K).

Avulsion flooding

Elevated erosion rates and sediment deposition have heightened the risk of avulsions [M1; M2]. On 22nd May 2024, for example, the Nyamwamba breached its outer bank upstream of Kasese town, inundating Kiwa hot springs and displacing 5,389 people [M1] (Table 2).

Formatted: Font color: Black

Formatted: Normal, Border: Top: (No border), Bottom: (No border), Left: (No border), Right: (No border), Between : (No border), Tab stops: 7.96 cm, Centered + 15.92 cm, Right

300 *Flood-driven Interactions*

301 High flows during fluvial and debris floods damage engineered flood defences, increasing their own probabilities of future
302 breaches in self-perpetuating positive feedback (#5; #147; #20; Appendix H). At the same time, their elevated velocities and
303 turbulence generate shear stress and hydraulic action that trigger river erosion (#6; #15) and accretion (#8; #18, #19). GIS
304 analysis confirms that the years of greatest erosion (2013 and 2020) coincided with the largest flood events [M1; R1] (Sect.
305 3-debris flood events [M1; R1] (Sect. 3.4). Fluvial, avulsion and debris floods transport contaminants across urban and
306 agricultural landscapes, driving runoff pollution (#6*; Appendix L). Additionally, debris floods deliver mobilized sediment
307 directly into the river channel, promoting accretion and progressively altering channel geometry over time (#19) [M1; M2;
308 R1] (Figure 4).

309 **3.3 Landslides**

310 Landslides caused by lateral river erosion undercutting riverbanks and hillslopes (Jacobs et al., 2016) have accelerated since
311 the wildfire due to higher post-fire discharges and sediment loads [I1; M1; M2; R1]. In addition, the initial destruction and
312 exposure of formerly stable riverbanks during the wildfire and 2013 flood has worked to further increase the probability of
313 mass movement into the river [M1; G2]. Previously, graded banks of unconsolidated quaternary sediment were anchored by
314 climax vegetation. Now, vertical river cliffs/riverbanks are exposed to direct erosion and undercutting at sites throughout the
315 river's long profile. As one local government representative describes, "when the floodwaters come down, they remove soil
316 and grasses to expose more boulders, and then you will have a landslide" [G2]. This process is visible in Fig. 3c, where the
317 riverbanks on sections of the burned side are now steep, unvegetated cliffs/banks of exposed and unconsolidated glacial till.

318 *Landslide-driven Interactions*

319 Landslides increase the probability of fluvial flooding by filling the channel with sediment and reducing the river's discharge
320 capacity (#1621). Five respondents have also witnessed a mechanism of temporary landslide damming and bursting "in the
321 space of a few minutes" [M1] during high flow events, from which surges of sediment and discharge activate fluvial floods
322 and debris flows/floods [G1; M1; M2; R1; W1]. As one resident recalls: "suddenly, I heard a roar like a plane taking off at
323 Entebbe Airport. Two landslides cut off the river and created a dam behind it, then soon after there were entire trees pole
324 vaulting over the debris" [R1].

325
326 Five respondents describe landslides as being in a positive feedback process with erosion (through reciprocal interactions
327 #1723, #22 and #810), whereby landslides add load to the river, accelerating accretion and lateral erosion by diverting flow to
328 the riverbanks and causing/trigger further landslides [R1; M1; M2; I1; G2]. Landslides also trigger heavy metal pollution
329 through the rotational slumping of solid Co-Cu tailings at Kilembe Mines into the River Nyamwamba (#1824; Sect. 3.5).

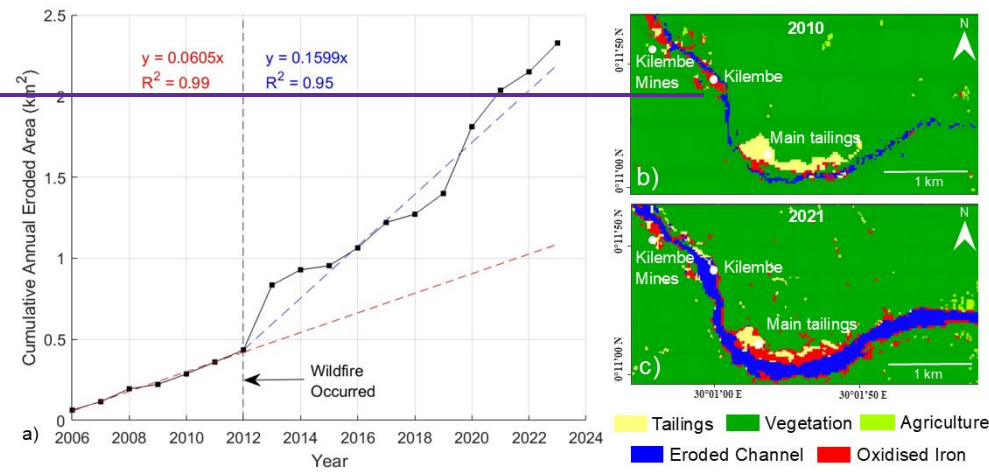
330

Formatted: Font color: Black

Formatted: Normal, Border: Top: (No border), Bottom: (No border), Left: (No border), Right: (No border), Between : (No border), Tab stops: 7.96 cm, Centered + 15.92 cm, Right

331 **3.4 River Channel Erosion and Accretion**

332 The cumulative annual eroded river channel area (Fig. 4a) shows a sustained increase in the river's rate of erosion by a factor
 333 of 2.64 following the 2012 wildfire, and the average middle-lower course channel width has increased sevenfold between 2010
 334 – 2021, from 16.9 m to 123 m. Rapid erosion has destroyed agricultural land [M1; M2; G1; G2], residential property, and
 335 critical road infrastructure [M1].



Formatted: Font color: Black

Formatted: Normal, Border: Top: (No border), Bottom: (No border), Left: (No border), Right: (No border), Between : (No border), Tab stops: 7.96 cm, Centered + 15.92 cm, Right

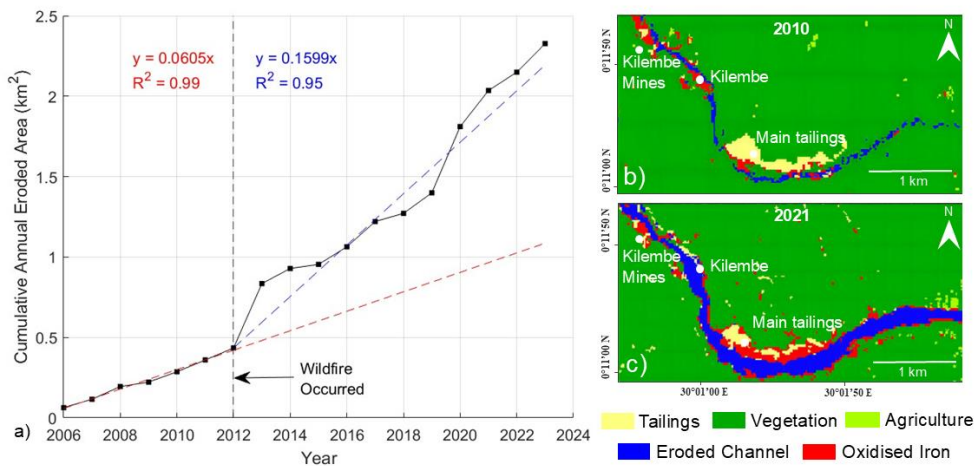


Figure 4: a) Annual cumulative eroded area in a 20 km mid-lower course section of the River Nyamwamba, calculated as the increase in eroded channel area between each year's supervised classification; b) supervised classification of a February 2010 Landsat-7 image; c) supervised classification of a February 2021 Landsat-8 image.

Erosion and Accretion-driven Interactions

Since the wildfire, accelerated lateral river channel erosion has both shifted the river channel closer to populated areas of Kasese town and reduced eroded debris has filled the channel via deposition, reducing its discharge capacity, thereby increasing. Together, these erosion and accretion processes increase the probability of urban flooding in Kasese town [R1; G1; G2; M2; I2; R3] (#7). Erosion and Accretion also increases the probability of avulsion flooding, as exemplified by the May and September 2024 floods, by filling the channel with sediment bars that divert flow towards riverbanks [M1] (#1213), whilst directly triggering avulsion floods when it breaks through unconsolidated banks [M1; M2] (#1414). Contributions of sediment to the main Nyamwamba channel also increase the probability of debris floods [M1; R1] (#1317).

Erosional undercutting destabilises slopes and directly triggers landslides (#810), consistent with Jacobs et al.'s (2016) mapping of 14 bank-failure slides during the May 2013 multi-hazard event. This lateral undercutting and exposure of vertical river cliffs/riverbanks is also described by three respondents as putting erosion in self-perpetuating positive feedback, by increasing the probability of further erosion at exposed banks [G1, G2, M1] (#911).

Erosion and accretion are also coupled through reciprocal feedback (#15, #16). Sediment deposition narrows the active channel cross-section, increasing the flow velocity and erosive potential (#15), driving further channel erosion. The eroded material

Formatted: Font: 9 pt, Bold, Font color: Black

Formatted: Normal, Space After: 10 pt, Border: Top: (No border), Bottom: (No border), Left: (No border), Right: (No border), Between : (No border)

Formatted: Font color: Black

Formatted: Normal, Border: Top: (No border), Bottom: (No border), Left: (No border), Right: (No border), Between : (No border), Tab stops: 7.96 cm, Centered + 15.92 cm, Right

358 [replenishes the sediment supply available for sediment deposition \(#16\), sustaining this cycle. Together, these dynamics place](#)
359 [erosion and accretion in a self-reinforcing feedback loop along the river’s reach.](#)

360
361 Channel widening breached the Kilembe mine copper-cobalt tailings deposit in 2014, ~~since~~ triggering heavy-metal pollution
362 downstream that now presents a major risk to public health (#1012; Sect. 3.5).
363

364 3.5 Pollution

365 Immediately after the 2012 wildfire, community members reported increased turbidity and a smell “*like methane*” [M1] in the
366 river. This is still reported during high discharge twelve years later, which four respondents believe to be due to runoff (non-
367 point source) pollution through exposed bogs and organic-rich glacial sediments in the fire-affected and eroding upper
368 catchment [M1; M2; R1; G1] (#1).
369

370 Beyond this diffuse pollution, accelerated river erosion (#1012) and landslides (#1824) have inputted an estimated 744,000
371 tonnes of a 15 Mt Kilembe Mines Co-Cu tailings deposit directly into the River Nyamwamba (mapped in Appendix K).
372 Satellite imagery and field photographs show erosional [cliffsbanks](#), slump scars and new channels within tailings areas, and
373 evidence of acid mine drainage from distinctive iron oxide precipitation (Fig. 3c; Appendix E). Elevated Co, Ni, Cu, Fe, Al,
374 S, Zn, As, Cd and Mn river contamination has previously been attributed to leaching of the Co-Cu mine (Abraham & Susan,
375 2017; Mwesigye et al., 2016; Mwesigye & Lawrence, 2024; Mwongyera et al., 2014).
376

377 Five respondents identified this solid waste pollution as a major concern for public health [M2; W1; G1; G2; R1]. The river is
378 used by 38% of its adjacent population for drinking, and by many more indirectly through crop-irrigation and groundwater
379 abstraction (Abraham and Susan, 2017; Mukisa et al., 2020). In addition to waterborne risks, long-term contamination of arable
380 soils by deposited mine waste raises concern for food safety [M1; M2; G1; G2]. As one Ministry of Water official noted, “*in*
381 *Kasese District, their teeth are turning brown with yellow patches, and we have been told that many people in this region are*
382 *ailing with cancer*” [M2]. Local environmental managers also expressed concern for downstream ecosystems in Queen
383 Elizabeth National Park and Lake George, where protected flora and fauna may be affected by the pollution and vegetation
384 dieback observed in Kasese town [G2; M1, R1, W1].

385 Pollution-driven Interactions

386 [Runoff pollution from the burned area transports elevated loads of fine sediment and contaminants into the river channel \(#1](#)
387 [\[M1; M2; R1; G1\]. This increased sediment supply promotes channel accretion as the excess sediment load settles into the](#)
388 [river channel \(#5\).](#)
389

Formatted: Font color: Black

Formatted: Normal, Border: Top: (No border), Bottom: (No border), Left: (No border), Right: (No border), Between : (No border), Tab stops: 7.96 cm, Centered + 15.92 cm, Right

4 Discussion: Implications for Management

The intensity and persistence of the Rwenzori hazard cascade highlights how wildfires in mature, fire-sensitive mountain ecosystems can impose long-lasting risks on downstream communities. ~~Unlike fire-adapted systems where vegetation recovers quickly to dampen hazard impacts, recovery~~ Recovery in these environments is slow, and positive feedback mechanisms sustain elevated risk. By characterising hazard interactions in full, this study identifies entry points for intervention. ~~Management as~~ management approaches that systematically impede hazard interactions can help unravel cascades (Gill and Malamud, 2016).

The principal way to impede this cascade is at the top (interactions #1-4), by promoting ecosystem recovery and attenuating the elevated runoff and river discharge driving other hazards. In the Rwenzori, authorities implemented a mix of hard engineering, community-centred and nature-based solutions ~~that in the lowlands which~~ has saved lives (see Appendix ~~L~~ ~~M~~); ~~however~~, the prevailing approach to wildfire restoration has been to await natural recovery. This passivity missed a critical window to implement soil stabilisation and runoff attenuation solutions such as mulching, contour felling and forest restoration (Papaioannou et al., 2023; Robichaud et al., 2013; Scheper et al., 2021), and allowed lower canopy vegetation to establish ahead of upper canopy tree species in the ericaceous zone (Fig. 3c). The challenge now is to develop recovery and discharge attenuation solutions in a partially recovered ecosystem. Addressing this requires post-wildfire expert assessment to guide restoration planning and build an evidence-base for financing solutions (Veness and Buytaert, 2025).

In the later stages of the Rwenzori cascade, erosion emerges as a key driver of multiple hazard interactions and positive feedback processes. It has accelerated landslides, amplified debris ~~flows~~ floods, triggered flooding, and caused a major water pollution hazard now requiring urgent investigation of its scale and health impacts. Stabilising riverbanks is a critical intervention to mitigate erosion and therefore impede its cascading interactions. We recommend integrating existing dredging, levee construction, and nature-based approaches to achieve this (Appendix ~~L~~ ~~M~~; MoWE, 2022). In particular, repositioning coarse sediment to riverbanks can help protect eroding ~~river cliffs~~ riverbanks, regrade unstable slopes, and create conditions for in-channel vegetation to anchor finer sediments and restore soil, thus mimicking the stable, unburned riverbank morphology seen in Fig. 3c (Sanches Fernandes et al., 2020). These measures are urgent in the mid-catchment to protect communities and limit further mobilisation of solid mine waste, but also advisable in the upper catchment to reduce sediment generation and landslide risk. ~~Developing an effective approach to bank stabilisation in the Rwenzori could serve as a blueprint for similar future events.~~

The principle of mimicking natural processes to promote post-wildfire recovery has been successfully implemented elsewhere (European Environment Agency, 2025). In New Mexico, Engineering With Nature (EWN) principles were implemented following the 2011 Las Conchas Wildfire to implement low-tech hillslope and in-channel structures including mulch barriers, contour-felled log debris, tree-check dams, and in-channel sediment grade-control features to stabilise slopes and reduce

423 [downstream sediment transport \(Haring et al., 2021\). In Arizona, USA, following the 2019 Museum Fire, alluvial fan](#)
424 [restoration through regrading and rock sill installation has a predicted reduction in downstream sediment transport of 70%](#)
425 [\(Schenk et al., 2025\). Post-fire restoration following the 2020 Cameron Peak Fire in Colorado included post-assisted log](#)
426 [structures and beaver dam analogues to attenuate peak flows and promote sediment aggradation in burned headwater streams](#)
427 [to replicate the hydrological buffering functions of pre-fire riparian systems \(Wheaton et al., 2019; CPRW, 2026; Nichter et](#)
428 [al., 2026\). Whilst these represent a small selection of examples, the underlying principle of designing interventions to mimic](#)
429 [pre-disturbance geomorphological and hydrological processes offers a transferable blueprint for post-wildfire management in](#)
430 [significantly altered catchments like the Nyamwamba \(Haring et al., 2021; Bombino et al., 2024\).](#)

431
432 Montane environments globally, especially those without a history of fire, require greater investment in monitoring and
433 research into post-wildfire hazard cascades (Arango Carmona et al. 2025; Wimberly et al. 2024). The lack of comparable case
434 studies makes it difficult to determine whether the Rwenzori represents an outlier or part of a broader emerging trend. ~~However,~~
435 [however](#), the intensity of the Rwenzori cascade, following a burn area of just 31 km², is a [warningsignal](#) to trigger post-fire
436 risk assessments at lower thresholds of burn area and severity when the fire occurs in a fire-sensitive mountain ecosystem.
437 Expanding research in similar regions will help build an evidence base of common cascading interactions and best practices
438 for their management.

439 5 Conclusions

440 This study has characterised a post-wildfire multi-hazard cascade in a tropical montane catchment, demonstrating how the
441 burning of a pristine, fire-sensitive mountain ecosystem can initiate cascading hazards of exceptional intensity and persistence.
442 As fire regimes continue to shift to higher altitudes under climate change, there is an emerging risk of similar hazard cascades
443 for downstream communities in tropical mountain catchments worldwide.

444
445 In Uganda's Rwenzori National Park, in the twelve years after a 2012 wildfire burned 31 km² of mature forest and peatland,
446 ten major floods with fluvial, debris or avulsion mechanisms occurred, with two debris floods requiring large-scale
447 humanitarian responses. Increased river discharge after the fire caused a 2.64-fold increase in erosion rates and increased the
448 probability of landslides, which have together driven a sevenfold increase in river channel width over nine years. Urban and
449 agricultural areas now face a real-time risk to public health due to the erosion and mass movement of 744,000 tonnes of copper-
450 cobalt solid tailings into the River Nyamwamba since 2014. This discrete escalation of hazards, interactions and impacts is
451 sustained by the slow recovery of vegetation poorly adapted to fire regimes, and multiple positive feedbacks between hazard
452 interactions.

Formatted: Font color: Black

Formatted: Normal, Border: Top: (No border), Bottom: (No border), Left: (No border), Right: (No border), Between : (No border), Tab stops: 7.96 cm, Centered + 15.92 cm, Right

454 The Rwenzori case highlights a need to recognise post-wildfire hazard cascades as a long-term risk in tropical mountain
455 environments, especially in newly fire-prone areas with no prior history of burning. [High-income countries generally have](#)
456 [established post-fire risk assessment protocols, such as the Burned Area Emergency Response used in the USA \(NICF, 2026\),](#)
457 [and the Post Wildfire Natural Hazard Risk Analysis in British Colombia, Canada \(Government of British Colombia, 2023\).](#)
458 [Meanwhile, many low- and middle-income countries still lack standardised assessment procedures at the local or national](#)
459 [level.](#) We recommend post-fire risk assessments and research, even for relatively small burn areas, when future fires occur in
460 previously unburned or fire sensitive mountain ecosystems. A better understanding of interactions between hazards identifies
461 intervention points, where interactions can be impeded through early actions that prevent ecosystem impacts from becoming
462 entrenched long-term. To this end, remediation of the burned zone should always be a priority to accelerate ecosystem recovery
463 and attenuate elevated runoff.

464
465 More monitoring and research of global case studies is needed to establish the prevalence and intensity of tropical mountain
466 wildfire hazard cascades, and best practices for their management. This study has additionally underscored the value of
467 integrating qualitative data and local knowledge into such studies. Interviews were critical to identifying key hazard
468 interactions that would not have been captured through physical or remote data alone. Interdisciplinary research, through close
469 partnerships between academic and local stakeholders, can improve collective visibility on this emerging climate risk and
470 accelerate the development of shared solutions.

471
472
473
474
475
476
477
478
479
480
481

482 **6 Data Availability**

483 The interview data is confidential according to ethical and data sharing restrictions. The GIS files are available on GitHub
484 (<https://github.com/will-veness/wildfires-uganda>) and will be available in Zenodo upon full publication.

Formatted: Font color: Black
Formatted: Normal, Border: Top: (No border), Bottom: (No border), Left: (No border), Right: (No border), Between : (No border), Tab stops: 7.96 cm, Centered + 15.92 cm, Right

485 **7 Competing Interests**

486 We declare no competing interests.

487 **8 Author Contributions**

488 William Veness: Writing – review & editing, Supervision, Writing – original draft, Visualization, Validation, Software, Resources, Project
489 administration, Methodology, Investigation, Funding acquisition, Formal analysis, Data curation, Conceptualization

490 Martha Day: Writing – review & editing, Writing – original draft, Visualization, Validation, Software, Resources, Methodology,
491 Investigation, Formal analysis, Data curation, Conceptualization

492 Anthony C. Ross: Writing – review & editing, Investigation, Data Curation, Validation

493 Yazidhi Bamutaze: Writing – review & editing, Funding acquisition, Data curation, Supervision, Investigation, Validation,
494 Conceptualization.

495 Jiayuan Han: Methodology, Investigation, Data Curation, Visualization, Software

496 Douglas Mulangwa: Project administration, Resources, Data curation, Investigation

497 Anthony Mwesigwa: Writing – review & editing, Project administration, Data curation, Investigation

498 Emmanuel Ntale: Project administration, Resources, Investigation

499 Callist Tindimugaya: Project administration, Resources, Methodology, Supervision, Conceptualization

500 Brian Guma: Project administration, Resources, Methodology, Investigation, Conceptualization, Supervision, Validation

501 Elisabeth Stephens: Writing – review & editing, Investigation, Project administration, Resources, Data Curation, Investigation, Validation

502 Wouter Buytaert: Writing – review & editing, Supervision, Methodology, Investigation, Project administration, Conceptualization,
503 Validation

504 **9 Acknowledgements**

505 We thank the Uganda Red Cross Society, the Ministry of Water and Environment, Kasese Municipality, and all local
506 collaborators and community members in Kasese District for their contributions to this research. We are grateful to the Uganda
507 Wildlife Authority and Rwenzori Trekking Services for facilitating access to the Rwenzori Mountains National Park. This
508 study was initiated through support from Imperial College London’s African Research Universities Alliance (ARUA)
509 partnership, which enabled collaboration with Makerere University. The Red Cross Red Crescent Climate Centre is also
510 gratefully acknowledged for its role in establishing the partnership with the Uganda Red Cross and the Ministry of Water and
511 Environment.

Formatted: Font color: Black

Formatted: Normal, Border: Top: (No border), Bottom: (No border), Left: (No border), Right: (No border), Between : (No border), Tab stops: 7.96 cm, Centered + 15.92 cm, Right

10 References

- Abraham, M. R., & Susan, T. B. (2017). Water contamination with heavy metals and trace elements from Kilembe copper mine and tailing sites in Western Uganda; implications for domestic water quality. *Chemosphere*, 169, 281–287. <https://doi.org/10.1016/j.chemosphere.2016.11.077>
- Act Alliance. (2013). *ACT Alliance Preliminary Appeal UGA131: Flash Floods in Kasese, Uganda* [Data set]. <https://reliefweb.int/report/uganda/act-alliance-preliminary-appeal-uga131-flash-floods-kasese-uganda>
- Act Alliance. (2020). *Uganda: Flood Emergency* (No. RRF No. 04/2020.) [Data set].
- AghaKouchak, A., Chiang, F., Huning, L. S., Love, C. A., Mallakpour, I., Mazdiyasi, O., Moftakhari, H., Papalexioi, S. M., Ragno, E., & Sadegh, M. (2020). Climate Extremes and Compound Hazards in a Warming World. *Annual Review of Earth and Planetary Sciences*, 48(1), 519–548. <https://doi.org/10.1146/annurev-earth-071719-055228>
- AghaKouchak, A., Huning, L. S., Chiang, F., Sadegh, M., Vahedifard, F., Mazdiyasi, O., Moftakhari, H., & Mallakpour, I. (2018). How do natural hazards cascade to cause disasters? *Nature*, 561(7724), 458–460. <https://doi.org/10.1038/d41586-018-06783-6>
- Ahmad, Z. U., Sakib, S., & Gang, D. D. (2016). Nonpoint Source Pollution. *Water Environment Research*, 88(10), 1594–1619. <https://doi.org/10.2175/106143016X14696400495497>
- Arango-Carmona, M. I., Voit, P., Hürlimann, M., Aristizábal, E., & Korup, O. (2025). *Hillslope-Torrential Hazard Cascades in Tropical Mountains*. Landslides and Debris Flows Hazards. <https://doi.org/10.5194/egusphere-2025-1698>
- Asiimwe, W. (2014). Kasese Hit Fresh Floods. *New Vision*. <https://newvision.co.ug/news/1341922/kasese-hit-fresh-floods>
- Belongia, M. F., Hammond Wagner, C., Seipp, K. Q., & Ajami, N. K. (2023). Building water resilience in the face of cascading wildfire risks. *Science Advances*, 9(37), eadf9534. <https://doi.org/10.1126/sciadv.adf9534>
- Bombino, G., D'Agostino, D., Marziliano, P. A., Pérez Cutillas, P., Praticò, S., Proto, A. R., Manti, L. M., Lofaro, G., & Zimbone, S. M. (2024). A Nature-Based Approach Using Felled Burnt Logs to Enhance Forest Recovery Post-Fire and Reduce Erosion Phenomena in the Mediterranean Area. *Land*, 13(2), 236. <https://doi.org/10.3390/land13020236>
- Boyer, E. W., Wagenbrenner, J. W., & Zhang, L. (2022). Wildfire and hydrological processes. *Hydrological Processes*, 36(7), e14640. <https://doi.org/10.1002/hyp.14640>
- British Geological Survey (2024) How to classify a landslide. British Geological Survey. Available at: <https://www.bgs.ac.uk/discovering-geology/earth-hazards/landslides/how-to-classify-a-landslide/#flows> (Accessed: 24 April 2026).
- Church, M., & Jakob, M. (2020). What Is a Debris Flood? *Water Resources Research*, 56(8), e2020WR027144. <https://doi.org/10.1029/2020WR027144>
- Coconino County Flood Control District. (no date). Alluvial Fan Stabilization Project. Coconino County, Arizona. Available at: <https://www.coconino.az.gov/2407/Alluvial-Fan-Stabilization-Project> (Accessed: 12 April 2026).

Formatted: English (United Kingdom)

Formatted: Font color: Black

Formatted: Normal, Border: Top: (No border), Bottom: (No border), Left: (No border), Right: (No border), Between : (No border), Tab stops: 7.96 cm, Centered + 15.92 cm, Right

- 559 [Coalition for the Poudre River Watershed \(CPRW\). \(no date\). Low-Tech Process-Based Restoration. Available at:](https://www.poudrewatershed.org/tpbr)
560 <https://www.poudrewatershed.org/tpbr> (Accessed: 12 April 2026).
- 561
- 562 Congedo, L. (2021). Semi-Automatic Classification Plugin: A Python tool for the download and processing of remote sensing
563 images in QGIS. *Journal of Open Source Software*, 6(64), 3172.
564 <https://doi.org/10.21105/joss.03172><https://doi.org/10.21105/joss.03172>
- 565
- 566 Copernicus Climate Change Service (C3S). (2017). ERA5: Fifth generation of ECMWF atmospheric reanalyses of the global
567 climate [Dataset]. Copernicus Climate Change Service Climate Data Store (CDS). <https://doi.org/10.1002/qj.3803>
- 568
- 569 [Costa, J.E. and Schuster, R.L. \(1987\) The formation and failure of natural dams. Open-File Report 87-392. Vancouver,](https://pubs.usgs.gov/of/1987/0392/report.pdf)
570 [Washington: U.S. Geological Survey. Available at: https://pubs.usgs.gov/of/1987/0392/report.pdf](https://pubs.usgs.gov/of/1987/0392/report.pdf) (Accessed: 24 April 2026).
- 571
- 572 Creswell, J., W. (2009). *Research Design: Qualitative, Quantitative and Mixed Methods Approaches* (Third Edition).
573 https://www.ucg.ac.me/skladiste/blog_609332/objava_105202/fajlovi/Creswell.pdfhttps://www.ucg.ac.me/skladiste/blog_609332/objava_105202/fajlovi/Creswell.pdf
- 574
- 575
- 576 [Cruden, D.M., Varnes, D.J. \(1996\) Landslide Types and Processes. Transportation Research Board, U.S. National Academy of](https://pubs.usgs.gov/of/1996/0392/report.pdf)
577 [Sciences. Special Report. 247: 36-75](https://pubs.usgs.gov/of/1996/0392/report.pdf)
- 578
- 579 DeBano, L. F. (2000). The role of fire and soil heating on water repellency in wildland environments: A review. *Journal of*
580 *Hydrology*, 231–232, 195–206. [https://doi.org/10.1016/S0022-1694\(00\)00194-3](https://doi.org/10.1016/S0022-1694(00)00194-3)[https://doi.org/10.1016/S0022-](https://doi.org/10.1016/S0022-1694(00)00194-3)
581 [1694\(00\)00194-3](https://doi.org/10.1016/S0022-1694(00)00194-3)
- 582
- 583 Delforge, D., Wathélet, V., Below, R., Lanfredi Sofia, C., Tonnelier, M., van Loenhout, J. A. F., & Speybroeck, N. (2025).
584 *EM-DAT: The Emergency Events Database, International Journal of Disaster Risk Reduction* (No. 105509) [Data set].
585 <https://doi.org/10.1016/j.ijdr.2025.105509><https://doi.org/10.1016/j.ijdr.2025.105509><https://doi.org/10.1016/j.ijdr.2025.105509>
- 586
- 587 DesInventar. (2025). *DesInventar Database* [Data set]. UNDRR. <https://www.desinventar.net/><https://www.desinventar.net/>
- 588
- 589 Doerr, S. H., Shakesby, R. A., & Walsh, R. P. D. (2000). Soil water repellency: Its causes, characteristics and hydro-
590 geomorphological significance. *Earth-Science Reviews*, 51(1–4), 33–65. [https://doi.org/10.1016/S0012-8252\(00\)00011-](https://doi.org/10.1016/S0012-8252(00)00011-8)
591 [8](https://doi.org/10.1016/S0012-8252(00)00011-8)[https://doi.org/10.1016/S0012-8252\(00\)00011-8](https://doi.org/10.1016/S0012-8252(00)00011-8)
- 592
- 593 Encalada, A. C., Flecker, A. S., Poff, N. L., Suárez, E., Herrera-R, G. A., Ríos-Touma, B., Jumani, S., Larson, E. I., &
594 Anderson, E. P. (2019). A global perspective on tropical montane rivers. *Science*, 365(6458), 1124–1129.
595 <https://doi.org/10.1126/science.aax1682><https://doi.org/10.1126/science.aax1682>
- 596
- 597
- 598 [European Environment Agency. \(2025\). Nature-based solutions for fire-resilient European forests. Publications Office of the](https://doi.org/10.2800/8810870)
599 [European Union. https://doi.org/10.2800/8810870](https://doi.org/10.2800/8810870)
- 600
- 601 [FAO. 2024. Integrated fire management voluntary guidelines – Principles and strategic actions. Second edition. Forestry](https://doi.org/10.4060/cd1090en)
602 [Working Paper, No. 41. Rome. https://doi.org/10.4060/cd1090en](https://doi.org/10.4060/cd1090en)
- 603
- 604 [FAO, & UNEP. \(2020\). The State of the World's Forests 2020 \[Table 6\]. FAO and UNEP. https://doi.org/10.4060/ca8642en](https://doi.org/10.4060/ca8642en)
605 [Flood List News. \(2020a\). Uganda – 8 Dead After More Floods in Kasese. Flood List. https://floodlist.com/africa/uganda-](https://doi.org/10.4060/ca8642en)
606 [floods-kasese-may-2020](https://floodlist.com/africa/uganda-floods-kasese-may-2020)<https://floodlist.com/africa/uganda-floods-kasese-may-2020>
- 607
- 608 [FAO and UNEP. \(2021\). Global assessment of soil pollution: Report. https://doi.org/10.4060/cb4894en](https://doi.org/10.4060/cb4894en)

Formatted: Font color: Black

Formatted: Normal, Border: Top: (No border), Bottom: (No border), Left: (No border), Right: (No border), Between : (No border), Tab stops: 7.96 cm, Centered + 15.92 cm, Right

607
608 Flood List News. (2020b). Uganda – Thousands Affected by Floods in Western Region. *Flood List*.
609 <https://floodlist.com/africa/uganda-thousands-affected-by-floods-in-western-region>
610 <https://floodlist.com/africa/uganda-thousands-affected-by-floods-in-western-region>
611
612 Galletta, A. (2020). *Mastering the Semi-Structured Interview and Beyond: From Research Design to Analysis and Publication*.
613 New York University Press.
614 <https://doi.org/10.18574/nyu/9780814732939.001.0001>
615
616 Gearon, J., Martin, H. K., DeLisle, C., Barefoot, E. A., Mohrig, D., Paola, C., & Edmonds, D. A. (2024). Rules of River
617 Avulsion Supplementary Data Files (Version 0.0.2) [Data set]. Zenodo. <https://doi.org/10.5281/ZENODO.10338685>
618
619 Gill, J. C., & Malamud, B. D. (2016). Hazard interactions and interaction networks (cascades) within multi-
620 hazard methodologies. *Earth System Dynamics*, 7(3), 659–679. [https://doi.org/10.5194/esd-7-659-](https://doi.org/10.5194/esd-7-659-2016)
621 [2016](https://doi.org/10.5194/esd-7-659-2016)
622
623 Google News. (2025). *Google News Search* [Data set]. Google News. [https://news.google.com/home?hl=en-](https://news.google.com/home?hl=en-GB&gl=GB&ccid=GB:en)
624 <https://news.google.com/home?hl=en-GB&gl=GB&ccid=GB:en>
625
626 Government of British Columbia. (2023). *Post wildfire natural hazard risk analysis*.
627 [https://www2.gov.bc.ca/gov/content/safety/wildfire-status/recovery/wildfire-land-based-recovery/post-wildfire-natural-](https://www2.gov.bc.ca/gov/content/safety/wildfire-status/recovery/wildfire-land-based-recovery/post-wildfire-natural-hazard-risk-analysis#PWFNHRA)
628 [hazard-risk-analysis#PWFNHRA](https://www2.gov.bc.ca/gov/content/safety/wildfire-status/recovery/wildfire-land-based-recovery/post-wildfire-natural-hazard-risk-analysis#PWFNHRA) Accessed 10th April 2026.
629
630 Guerriero, L., Tufano, R., Capozzi, V., Budillon, G., Di Muro, C., Esposito, L., Forte, G., Vitale, E., & Calcaterra, D. (2025).
631 A postwildfire debris flood in Gragnano, southern Italy, on September 11, 2024. *Landslides*, 22(6), 1923–1936.
632 <https://doi.org/10.1007/s10346-025-02509-8>
633
634 Haring, C. P., Altmann, G. L., Suedel, B. C., & Brown, S. W. (2021). Using Engineering With Nature® (EWN®) principles
635 to manage erosion of watersheds damaged by large-scale wildfires. *Integrated Environmental Assessment and Management*,
636 17(6), 1194–1202. <https://doi.org/10.1002/ieam.4453>
637
638 Hasanuzzaman, M., Islam, A., Bera, B., & Shit, P. K. (2024). Quantifying the riverbank erosion and accretion rate using DSAS
639 model study from the lower Ganga River, India. *Natural Hazards Research*, 4(4), 550–561.
<https://doi.org/10.1016/j.nhres.2023.12.015>
640
641 Hinzmann, A., Mölg, T., Braun, M., Cullen, N. J., Hardy, D. R., Kaser, G., & Prinz, R. (2024). Tropical glacier loss in East
642 Africa: Recent areal extents on Kilimanjaro, Mount Kenya, and in the Rwenzori Range from high-resolution remote sensing
data. *Environmental Research: Climate*, 3(1), 011003. <https://doi.org/10.1088/2752-5295/ad1fd7>
643
644 Hungr, O., Leroueil, S., & Picarelli, L. (2014). The Varnes classification of landslide types, an update. *Landslides*, 11(2), 167–
645 194. <https://doi.org/10.1007/s10346-013-0436-y>
646
647 Islam, A., & Guchhait, S. K. (2020). Characterizing cross-sectional morphology and channel inefficiency of lower Bhagirathi
648 River, India, in post-Farakka barrage condition. *Natural Hazards*, 103(3), 3803–3836. [https://doi.org/10.1007/s11069-020-](https://doi.org/10.1007/s11069-020-04156-9)
649 [04156-9](https://doi.org/10.1007/s11069-020-04156-9)
650
651 Jacobs, L., Maes, J., Mertens, K., Sekajugo, J., Thiery, W., Van Lipzig, N., Poesen, J., Kervyn, M., & Dewitte, O. (2016).
652 Reconstruction of a flash flood event through a multi-hazard approach: Focus on the Rwenzori Mountains, Uganda. *Natural*
653 *Hazards*, 84(2), 851–876. <https://doi.org/10.1007/s11069-016-2458-y>
<https://doi.org/10.1007/s11069-016-2458-y>

Formatted: Font color: Black

Formatted: Normal, Border: Top: (No border), Bottom: (No border), Left: (No border), Right: (No border), Between : (No border), Tab stops: 7.96 cm, Centered + 15.92 cm, Right

654 Jordan, P. (2016). Post-wildfire debris flows in southern British Columbia, Canada. *International Journal of Wildland Fire*,
655 25(3), 322. <https://doi.org/10.1071/WF14070><https://doi.org/10.1071/WF14070>

656

657 Juma, B. (2016). Uganda – At Least 1,000 Displaced After Floods in Kasese and Kampala. *Flood List*.
658 [https://floodlist.com/africa/uganda-1000-](https://floodlist.com/africa/uganda-1000-displaced-floods-kasese-kampala)
659 [displaced-floods-kasese-kampala](https://floodlist.com/africa/uganda-1000-displaced-floods-kasese-kampala)

660

661 Kappelle, M., Geuze, T., Leal, M. E., & Cleef, A. M. (1996). Successional age and forest structure in a Costa Rican upper
662 montane *Quercus* forest. *Journal of Tropical Ecology*, 12(5), 681–698.
663 <https://doi.org/10.1017/S0266467400009871><https://doi.org/10.1017/S0266467400009871>

664

665 Kemter, M., Fischer, M., Luna, L. V., Schönfeldt, E., Vogel, J., Banerjee, A., Korup, O., & Thonicke, K. (2021). Cascading
666 Hazards in the Aftermath of Australia’s 2019/2020 Black Summer Wildfires. *Earth’s Future*, 9(3), e2020EF001884.
667 <https://doi.org/10.1029/2020EF001884><https://doi.org/10.1029/2020EF001884>

668

669 Key, C. H., & Benson, N. C. (2006). *Landscape Assessment (LA)*.

670

671 [Korup, O., and Schlunegger, F. \(2007\). Bedrock landsliding, river incision, and transience of geomorphic hillslope-channel](https://doi.org/10.1029/2006JF000710)
672 [coupling: Evidence from inner gorges in the Swiss Alps. *Journal of Geophysical Research: Earth Surface*, 112\(F3\),](https://doi.org/10.1029/2006JF000710)
673 [2006JF000710. <https://doi.org/10.1029/2006JF000710>](https://doi.org/10.1029/2006JF000710)

674

675 [Lawler, D. M. \(1993\). The measurement of river bank erosion and lateral channel change: A review. *Earth Surface Processes*
676 \[and Landforms\]\(https://doi.org/10.1002/esp.3290180905\), 18\(9\), 777–821. <https://doi.org/10.1002/esp.3290180905>](https://doi.org/10.1002/esp.3290180905)

677

678 Marengo, J. A., Cunha, A. P., Cuartas, L. A., Deusdará Leal, K. R., Broedel, E., Seluchi, M. E., Michelin, C. M., De Praga
679 Baião, C. F., Chuchón Angulo, E., Almeida, E. K., Kazmierczak, M. L., Mateus, N. P. A., Silva, R. C., & Bender, F. (2021).
680 Extreme Drought in the Brazilian Pantanal in 2019–2020: Characterization, Causes, and Impacts. *Frontiers in Water*, 3,
681 639204. <https://doi.org/10.3389/frwa.2021.639204><https://doi.org/10.3389/frwa.2021.639204>

682

683 Maxar Technologies. (2025a). *Historical satellite imagery from March 2006 of Kilembe, Uganda via Google Earth Pro* [Data
684 set]. Google Earth Pro.

685

686 Maxar Technologies. (2025b). *Satellite imagery from 10th April 2023 of Kilembe, Uganda via Bing Maps* [Data set]. Bing
687 Maps. <https://www.bing.com/maps><https://www.bing.com/maps>

688

689 McCaffrey, S. (2004). Thinking of Wildfire as a Natural Hazard. *Society & Natural Resources*, 17(6), 509–516.
690 <https://doi.org/10.1080/08941920490452445><https://doi.org/10.1080/08941920490452445>

691

692 [McGuire, L.A., Ebel, B.A., Rengers, F.K. et al. Fire effects on geomorphic processes. *Nat Rev Earth Environ* 5, 486–503](https://doi.org/10.1038/s43017-024-00557-7)
693 [\(2024\). <https://doi.org/10.1038/s43017-024-00557-7>](https://doi.org/10.1038/s43017-024-00557-7)

694

695 McKee, T.B., Doesken, N.J. and Kleist, J. (1993) The Relationship of Drought Frequency and Duration to Time Scales. 8th
696 Conference on Applied Climatology, Anaheim, 17-22 January 1993, 179-184.

697

698 Mojtahed, R., Nunes, M. B., Martins, J. T., & Peng, A. (2014). *Equipping the Constructivist Researcher: The Combined use*
699 *of Semi-Structured Interviews and Decision-Making maps*. 12(2).

700

701 [Moody, J. A., & Martin, D. A. \(2001\). Initial hydrologic and geomorphic response following a wildfire in the Colorado Front](https://doi.org/10.1002/esp.253)
[Range. *Earth Surface Processes and Landforms*, 26\(10\), 1049–1070. <https://doi.org/10.1002/esp.253>](https://doi.org/10.1002/esp.253)

Formatted: Font color: Black

Formatted: Normal, Border: Top: (No border), Bottom: (No border), Left: (No border), Right: (No border), Between : (No border), Tab stops: 7.96 cm, Centered + 15.92 cm, Right

- 702 MoWE (2022). INTEGRATED WATER MANAGEMENT AND DEVELOPMENT PROJECT; IMPLEMENTATION OF
703 PRIORITY CATCHMENT MANAGEMENT MEASURES IN MIDSTREAM NYAMWAMBA (No. P163782). Uganda
704 Ministry of Water and Environment.
705
- 706 [Muhamud, N. W., & Joyfred, A. \(2015\). Socio-Economic Factors Assessment Affecting the Adoption of Soil Conservation
707 Technologies on Rwenzori Mountain \[Table 1\]. *Indonesian Journal of Geography*, 47\(1\), 26. <https://doi.org/10.22146/ijg.6743>](#)
- 708 Mukisa, W., Yatuha, J., Andama, M., & Kasangaki, A. (2020). Heavy metal pollution in the main rivers of Rwenzori Region,
709 Kasese District, South-Western Uganda. *Oct. Jour. Env. Res.* 8(3).
710
- 711 Mwesigye, A. R., & Lawrence, O. B. (2024). Trace Elements Contamination of Kilembe Copper Mine Catchment Soils in
712 Kasese District, Western Uganda. *Soil and Sediment Contamination: An International Journal*, 33(2), 232–243.
713 <https://doi.org/10.1080/15320383.2023.2195512><https://doi.org/10.1080/15320383.2023.2195512>
- 714
- 715 Mwesigye, A. R., Young, S. D., Bailey, E. H., & Tumwebaze, S. B. (2016). Population exposure to trace elements in the
716 Kilembe copper mine area, Western Uganda: A pilot study. *Science of The Total Environment*, 573, 366–375.
717 <https://doi.org/10.1016/j.scitotenv.2016.08.125><https://doi.org/10.1016/j.scitotenv.2016.08.125>
- 718
- 719 Mwongyera, A., Mbabazi, J., Muwanga, A., Ntale, M., & Kwetegyeka, J. (2014). Impactof the disused Kilembe mine pyrites
720 on the domestic water quality of Kasese town, western Uganda. *Caribbean Journal of Science and Technology (CJST)*, 2, 482–
721 495.
722
- 723 [National Interagency Fire Centre \(NICE\). \(2026\). *Post Fire Recovery*. <https://www.nifc.gov/programs/post-fire-recovery>
724 \(Accessed 10th April 2026\).](#)
- 725
- 726 [New Vision. \(2024\). *Kasese PWDs bear the brunt of floods, landslides*. \[https://www.newvision.co.ug/category/news/kasese-
727 pwds-bear-the-brunt-of-floods-landslid-NV-188969\]\(https://www.newvision.co.ug/category/news/kasese-pwds-bear-the-brunt-of-floods-landslid-NV-188969\)\[https://www.newvision.co.ug/category/news/kasese-pwds-bear-the-
729 brunt-of-floods-landslid-NV-188969\]\(https://www.newvision.co.ug/category/news/kasese-pwds-bear-the-
728 brunt-of-floods-landslid-NV-188969\)](#)
- 730
- 731 [Nichter, K. A., Gilmore, T., Carbone, C., Sellers, B., Fairchild, M. P., & Preston, D. L. \(2026\). Ecological Characteristics of
732 Stream Reaches With and Without Low-Tech Process-Based Restoration in a Wildfire-Affected Catchment. *River Research
733 and Applications*, rra.70119. <https://doi.org/10.1002/rra.70119>](#)
- 734
- 735 Norville, C., Ivory, S., Russell, J. M., Mason, A., Nakileza, B., & Miller, J. (2024, December). *Using charcoal to calibrate the
736 frequency of wildfire in the Rwenzori Mountains over the Holocene* [Conference poster]. AGU Fall Meeting 2024, Washington,
737 DC, United States.
- 738
- 739 [Obando-Cabrera, L., Díaz-Timoté, J. J., Bastarrika, A., Celis, N., & Hantson, S. \(2025\). The Paramo Fire Atlas: Quantifying
740 burned area and trends across the Tropical Andes. *Environmental Research Letters*, 20\(5\), 054019.
741 <https://doi.org/10.1088/1748-9326/adc8ba><https://doi.org/10.1088/1748-9326/adc8ba>](#)
- 742
- 743 [Okiror, S. \(2020\). ‘People are desperate’: Floods and rock slides devastate western Uganda. *The Guardian*.
744 \[https://www.theguardian.com/global-development/2020/may/16/people-are-desperate-floods-and-rock-slides-devastate-
745 western-uganda\]\(https://www.theguardian.com/global-development/2020/may/16/people-are-desperate-floods-and-rock-slides-devastate-western-uganda\)\[https://www.theguardian.com/global-development/2020/may/16/people-are-desperate-floods-and-rock-
747 slides-devastate-western-uganda\]\(https://www.theguardian.com/global-development/2020/may/16/people-are-desperate-floods-and-rock-
746 slides-devastate-western-uganda\)](#)
- 747
- 748 [Oliveras, I., Malhi, Y., Salinas, N., Huaman, V., Urquiaga-Flores, E., Kala-Mamani, J., Quintano-Loaiza, J. A., Cuba-Torres,
I., Lizarraga-Morales, N., & Román-Cuesta, R.-M. \(2014\). Changes in forest structure and composition after fire in tropical](#)

Formatted: Font color: Black

Formatted: Normal, Border: Top: (No border), Bottom: (No border), Left: (No border), Right: (No border), Between : (No border), Tab stops: 7.96 cm, Centered + 15.92 cm, Right

749 montane cloud forests near the Andean treeline. *Plant Ecology & Diversity*, 7(1–2), 329–340.
750 <https://doi.org/10.1080/17550874.2013.816800><https://doi.org/10.1080/17550874.2013.816800>

751

752 Ometto, J. P., Kalaba, K., Anshari, G. Z., Chacon, N., Farrell, A., Halim, S. A., Neufeldt, H., & Sukumar, R. (2022). *Cross-*
753 *Chapter Paper 7: Tropical Forests. In: Climate Change 2022 – Impacts, Adaptation and Vulnerability: Working Group II*
754 *Contribution to the Sixth Assessment Report of the Intergovernmental Panel on Climate Change* (1st edn). Cambridge
755 University Press. <https://doi.org/10.1017/9781009325844.024><https://doi.org/10.1017/9781009325844.024>

756

757 Papaioannou, G., Alamanos, A., & Maris, F. (2023). Evaluating Post-Fire Erosion and Flood Protection Techniques: A
758 Narrative Review of Applications. *GeoHazards*, 4(4), 380–405.
759 <https://doi.org/10.3390/geohazards4040022><https://doi.org/10.3390/geohazards4040022>

760

761 Paton, D. (2003). Disaster preparedness: A social-cognitive perspective. *Disaster Prevention and Management: An*
762 *International Journal*, 12(3), 210–216.
763 <https://doi.org/10.1108/09653560310480686><https://doi.org/10.1108/09653560310480686>

764

765 Patton, M. Q. (2014). *Qualitative Research & Evaluation Methods* (Fourth Edition). SAGE Publications, Inc.
766 <https://us.sagepub.com/en-us/nam/qualitative-research-evaluation-methods/book232962>[https://us.sagepub.com/en-](https://us.sagepub.com/en-us/nam/qualitative-research-evaluation-methods/book232962)
767 [us/nam/qualitative-research-evaluation-methods/book232962](https://us.sagepub.com/en-us/nam/qualitative-research-evaluation-methods/book232962)

768

769 Pivello, V. R., Vieira, I., Christianini, A. V., Ribeiro, D. B., Da Silva Menezes, L., Berlinck, C. N., Melo, F. P. L., Marengo,
770 J. A., Tornquist, C. G., Tomas, W. M., & Overbeck, G. E. (2021). Understanding Brazil’s catastrophic fires: Causes,
771 consequences and policy needed to prevent future tragedies. *Perspectives in Ecology and Conservation*, 19(3), 233–255.
772 <https://doi.org/10.1016/j.pecon.2021.06.005><https://doi.org/10.1016/j.pecon.2021.06.005>

773

774 ReliefWeb. (2024). Uganda—Floods (DG ECHO Partners, Uganda Red Cross, media) (ECHO Daily Flash of 10 September
775 2024)—Uganda. In *ReliefWeb*.

776

777 Rengers, F. K., McGuire, L. A., Oakley, N. S., Kean, J. W., Staley, D. M., & Tang, H. (2020). Landslides after wildfire:
778 Initiation, magnitude, and mobility. *Landslides*, 17(11), 2631–2641. [https://doi.org/10.1007/s10346-020-01506-](https://doi.org/10.1007/s10346-020-01506-3)
779 [3](https://doi.org/10.1007/s10346-020-01506-3)<https://doi.org/10.1007/s10346-020-01506-3>

780

781

782 Ring, U. (2008). Extreme uplift of the Rwenzori Mountains in the East African Rift, Uganda: Structural framework and
783 possible role of glaciations. *Tectonics*, 27(4), 2007TC002176. <https://doi.org/10.1029/2007TC002176>

784

785 Robichaud, P. R., Lewis, S. A., Wagenbrenner, J. W., Ashmun, L. E., & Brown, R. E. (2013). Post-fire mulching for runoff
786 and erosion mitigation. *CATENA*, 105, 75–92.
787 <https://doi.org/10.1016/j.catena.2012.11.015><https://doi.org/10.1016/j.catena.2012.11.015>

788

789 Rudoy, A. N. (2002). Glacier-dammed lakes and geological work of glacial superfloods in the Late Pleistocene, Southern
790 Siberia, Altai Mountains. *Quaternary International*, 87(1), 119–140. [https://doi.org/10.1016/S1040-6182\(01\)00066-0](https://doi.org/10.1016/S1040-6182(01)00066-0)

791

792 Saldana, J. (2021). *The Coding Manual for Qualitative Researchers*. [https://us.sagepub.com/en-us/nam/the-coding-manual-](https://us.sagepub.com/en-us/nam/the-coding-manual-for-qualitative-researchers/book273583)
793 [for-qualitative-researchers/book273583](https://us.sagepub.com/en-us/nam/the-coding-manual-for-qualitative-researchers/book273583)[https://us.sagepub.com/en-us/nam/the-coding-manual-](https://us.sagepub.com/en-us/nam/the-coding-manual-for-qualitative-researchers/book273583)
794 [researchers/book273583](https://us.sagepub.com/en-us/nam/the-coding-manual-for-qualitative-researchers/book273583)

Formatted: Font color: Black

Formatted: Normal, Border: Top: (No border), Bottom: (No border), Left: (No border), Right: (No border), Between : (No border), Tab stops: 7.96 cm, Centered + 15.92 cm, Right

795 Salinas, N., Cosio, E. G., Silman, M., Meir, P., Nottingham, A. T., Roman-Cuesta, R. M., & Malhi, Y. (2021). Editorial:
796 Tropical Montane Forests in a Changing Environment. *Frontiers in Plant Science*, *12*, 712748.
797 <https://doi.org/10.3389/fpls.2021.712748><https://doi.org/10.3389/fpls.2021.712748>
798

799 Sanches Fernandes, L. F., Sampaio Pinto, A. A., Salgado Terêncio, D. P., Leal Pacheco, F. A., & Vitor Cortes, R. M. (2020).
800 Combination of Ecological Engineering Procedures Applied to Morphological Stabilization of Estuarine Banks after Dredging.
801 *Water*, *12*(2), 391. <https://doi.org/10.3390/w12020391><https://doi.org/10.3390/w12020391>
802

803 Sandwell, D., Anderson, D. L., & Wessel, P. (2005). Global tectonic maps. In G. R. Foulger, J. H. Natland, D. C. Presnall, &
804 D. L. Anderson, *Plates, plumes and paradigms*. Geological Society of America. [https://doi.org/10.1130/0-8137-2388-](https://doi.org/10.1130/0-8137-2388-4)
805 [4](https://doi.org/10.1130/0-8137-2388-4)[https://doi.org/10.1130/0-8137-2388-4.1](https://doi.org/10.1130/0-8137-2388-4)
806

807 Saunders, M., Lewis, P., & Thornhill, A. (2016). *Research methods for business students* (7th edition). Pearson.
808

809 [Schenk, E. R., Wood, A., Haden, A., Baca, G., Fleishman, J., & Loverich, J. \(2025\). Post-wildfire sediment source and](https://doi.org/10.5194/nhess-25-727-2025)
810 [transport modeling, empirical observations, and applied mitigation: An Arizona, USA, case study. *Natural Hazards and Earth*](https://doi.org/10.5194/nhess-25-727-2025)
811 [System Sciences](https://doi.org/10.5194/nhess-25-727-2025), *25*(2), 727–745. <https://doi.org/10.5194/nhess-25-727-2025>

812 Scheper, A. C., Verweij, P. A., & Van Kuijk, M. (2021). Post-fire forest restoration in the humid tropics: A synthesis of
813 available strategies and knowledge gaps for effective restoration. *Science of The Total Environment*, *771*, 144647.
814 <https://doi.org/10.1016/j.scitotenv.2020.144647><https://doi.org/10.1016/j.scitotenv.2020.144647>
815

816 Shakesby, R. A., & Doerr, S. H. (2006). Wildfire as a hydrological and geomorphological agent. *Earth-Science Reviews*, *74*(3–
817 4), 269–307. <https://doi.org/10.1016/j.earscirev.2005.10.006>
818

819 Sklar, L. S., & Dietrich, W. E. (2001). Sediment and rock strength controls on river incision into bedrock. *Geology*, *29*, 1087.
820 [https://doi.org/10.1130/0091-7613\(2001\)029%253C1087:SARSCO%253E2.0.CO;2](https://doi.org/10.1130/0091-7613(2001)029%253C1087:SARSCO%253E2.0.CO;2)

821 Slingerland, R., & Smith, N. D. (2004). RIVER AVULSIONS AND THEIR DEPOSITS. *Annual Review of Earth and*
822 *Planetary Sciences*, *32*(1), 257–285. <https://doi.org/10.1146/annurev.earth.32.101802.120201>
823

824 Stock, J., & Dietrich, W. E. (2003). Valley incision by debris flows: Evidence of a topographic signature. *Water Resources*
825 *Research*, *39*(4), 2001WR001057. <https://doi.org/10.1029/2001WR001057>

826 Stooft, C. R., Vervoort, R. W., Iwema, J., Van Den Elsen, E., Ferreira, A. J. D., & Ritsema, C. J. (2012). Hydrological response
827 of a small catchment burned by experimental fire. *Hydrology and Earth System Sciences*, *16*(2), 267–285.
828 <https://doi.org/10.5194/hess-16-267-2012>
829

830 Swain, D. L., Prein, A. F., Abatzoglou, J. T., Albano, C. M., Brunner, M., Diffenbaugh, N. S., Singh, D., Skinner, C. B., &
831 Touma, D. (2025). Hydroclimate volatility on a warming Earth. *Nature Reviews Earth & Environment*, *6*(1), 35–50.
832 <https://doi.org/10.1038/s43017-024-00624-z><https://doi.org/10.1038/s43017-024-00624-z>
833

834 UNdata. (2026). UNdata Glossary: Nonpoint source pollution. Available at:
835 <https://data.un.org/Glossary.aspx?q=nonpoint+source+pollution> (Accessed: 24 April 2026)
836

837 UNDRR. (2025). Hazard Information Profiles. United Nations Office for Disaster Risk Reduction. Available at:
838 <https://www.preventionweb.net/drr-glossary/hips> (Accessed: 12 April 2026).
839

840 UNEP. (2022). *Spreading like wildfire—The rising threat of extraordinary landscape fires. A UNEP Rapid Response*
841 *Assessment*. United Nations Environment Programme.

Formatted: Font color: Black

Formatted: Normal, Border: Top: (No border), Bottom: (No border), Left: (No border), Right: (No border), Between : (No border), Tab stops: 7.96 cm, Centered + 15.92 cm, Right

842
843
844
845
846
847
848
849
850
851
852
853
854
855
856
857
858
859
860
861
862
863
864
865
866
867
868
869
870
871
872
873
874
875
876
877
878
879
880
881
882
883
884
885
886
887
888
889
890
891

UNESCO. (2012). State of conservation of World Heritage properties inscribed on the World Heritage List. WHC-12/36.COM/7B. Paris: United Nations Educational, Scientific and Cultural Organization. Available at: <https://whc.unesco.org/archive/2012/whc12-36com-7B-en.pdf> (Accessed: 12 April 2026).

UNESCO and WMO (Eds). (2012). *International glossary of hydrology: = Glossaire international d'hydrologie*. WMO.

Vahedifard, F., Abdollahi, M., Leshchinsky, B. A., Stark, T. D., Sadegh, M., & AghaKouchak, A. (2024). Interdependencies Between Wildfire-Induced Alterations in Soil Properties, Near-Surface Processes, and Geohazards. *Earth and Space Science*, 11(2), e2023EA003498. <https://doi.org/10.1029/2023EA003498><https://doi.org/10.1029/2023EA003498>

Veness, W. A., & Buytaert, W. (2025). Towards an evidence base for groundwater data investments. *Environmental Science & Policy*, 164, 104014. <https://doi.org/10.1016/j.envsci.2025.104014><https://doi.org/10.1016/j.envsci.2025.104014>

Wesche, K., Miehe, G. and Kaeppli, M. (2000) 'The Significance of Fire for Afroalpine Ericaceous Vegetation', *Mountain Research and Development*, 20(4), pp. 340–347. Available at: [https://doi.org/10.1659/0276-4741\(2000\)020\[0340:TSOFFA\]2.0.CO;2](https://doi.org/10.1659/0276-4741(2000)020[0340:TSOFFA]2.0.CO;2)

Williams, D. J. (2015). Placing Soil Covers on Soft Mine Tailings. In *Ground Improvement Case Histories* (pp. 51–81). Elsevier. <https://doi.org/10.1016/B978-0-08-100698-6.00002-7><https://doi.org/10.1016/B978-0-08-100698-6.00002-7>

Wimberly, M. C., Wanyama, D., Doughty, R., Peiro, H., & Crowell, S. (2024). Increasing Fire Activity in African Tropical Forests Is Associated With Deforestation and Climate Change. *Geophysical Research Letters*, 51(9), e2023GL106240. <https://doi.org/10.1029/2023GL106240><https://doi.org/10.1029/2023GL106240>

Formatted: Font color: Black

Formatted: Normal, Border: Top: (No border), Bottom: (No border), Left: (No border), Right: (No border), Between : (No border), Tab stops: 7.96 cm, Centered + 15.92 cm, Right

892 [Wheaton, J. M., Bennett, S. N., Bouwes, N., Maestas, J. D., & Shahverdian, S. \(2019\). Low-Tech Process-Based Restoration](#)
893 [of Riverscapes: Design Manual. Version 1.0. https://doi.org/10.13140/RG.2.2.19590.63049/2](#)

894 **11 Appendices**

895 **Appendix A: 1-Month Standardised Precipitation Index Calculation for January 2012**

896 [ERA5 monthly averaged reanalysis total precipitation data was downloaded from 1974 – 2024 for the pixel covering to the](#)
897 [burned area \(centroid coordinates: 0.4°N, 29.8°E; Copernicus Climate Change Service \(C3S\), 2017\). This was processed in](#)
898 [MATLAB following McKee et al.'s \(1993\) method to determine the monthly SPI for January 2012.](#)

899 [ERA5 monthly averaged reanalysis total precipitation data was downloaded from 1974 – 2024 for the pixel covering to the](#)
900 [burned area \(centroid coordinates: 0.4°N, 29.8°E; Copernicus Climate Change Service \(C3S\), 2017\). This was processed in](#)
901 [MATLAB following McKee et al.'s \(1993\) method to determine the monthly SPI for January 2012.](#)

903 **Appendix B: Eroded Tailings Volume Calculation**

904 The average original height of the tailings was calculated to be 23 m, assumed to be flat across the original dammed area,
905 which was calculated (32945 m²) from historic satellite imagery.

906
907 This average height (23 m) was multiplied by the eroded footprint area (m²) to get a volume, then volumetric subtractions were
908 made to account for the originally sloped (55 degrees) walls of the tailings dam and the wedges of slumped material yet to be
909 eroded at the foot of the collapsed tailings escarpments. The volume of these wedges was calculated from the slope angle and
910 height of their triangular cross-section, multiplied by their width parallel to the eroded tailings escarpment.

911
912 The tonnage of eroded tailings was then calculated by multiplying their estimated volume by their assumed average dry density
913 (1.5 t/m³) based on standard values for copper-cobalt tailings ([Williams, 2015](#));([Williams, 2015](#)).

915 **Appendix C: Semi-Structured Interview Template**

916 *Background*

- 917 ●● What organisation do you represent?
- 918 ●● What is your role?
- 919 ●● What is your experience of hazards in the Rwenzori?

921 *Perceptions of changing hazard risk*

Formatted: English (United Kingdom)

Formatted: Normal, Outline numbered + Level: 1 +
Numbering Style: Bullet + Aligned at: 0.63 cm + Indent at:
1.27 cm, Border: Top: (No border), Bottom: (No border), Left:
(No border), Right: (No border), Between : (No border)

Formatted: Font color: Black

Formatted: Normal, Border: Top: (No border), Bottom: (No
border), Left: (No border), Right: (No border), Between : (No
border), Tab stops: 7.96 cm, Centered + 15.92 cm, Right

- 922 ●● Do you feel the risk of hazards have changed (in the Nyamwamba catchment)? How?
- 923 ●● If yes, why do you feel risk is changing?
- 924 ●● Do you feel the river Nyamwamba/Mubuku/other rivers have changed?
- 925 ●● If yes, why do you think this change has happened?

Formatted: Normal, Outline numbered + Level: 1 + Numbering Style: Bullet + Aligned at: 0.63 cm + Indent at: 1.27 cm, Border: Top: (No border), Bottom: (No border), Left: (No border), Right: (No border), Between : (No border)

927 *Awareness and efficacy of existing management strategies*

- 928 ●● What existing strategies are in place to manage hazard risk in the Rwenzori?
- 929 ●● Do you feel these strategies are working?

Formatted: Normal, Outline numbered + Level: 1 + Numbering Style: Bullet + Aligned at: 0.63 cm + Indent at: 1.27 cm, Border: Top: (No border), Bottom: (No border), Left: (No border), Right: (No border), Between : (No border)

931 *Potential alternative management strategies*

- 932 ●● What strategies do you feel would better reduce hazard risk in the Rwenzori?
- 933 ●● Why do you think these have not been implemented yet?
- 934 ●● Do you feel nature-based solutions could be used to manage these hazards?

Formatted: Normal, Outline numbered + Level: 1 + Numbering Style: Bullet + Aligned at: 0.63 cm + Indent at: 1.27 cm, Border: Top: (No border), Bottom: (No border), Left: (No border), Right: (No border), Between : (No border)

936 **Appendix D: Evidence for The Multi-Hazard Cascade Interactions**

937 **Table D1**

Table D1: Definitions of hazard terminology in this article from the 2025 Hazard Information Profiles (HIPs; UNDRR, 2025).

*Both avulsion flooding and debris flooding are profiled under Flooding - MH0600 (UNDRR, 2025) however further distinction using key references between these types of flooding is important here for understanding the hazard cascade and its interactions.

<u>Hazard</u>	<u>HIPs 2025 Definition</u>	<u>HIP 2025 Identifier</u>	<u>Primary Source(s)</u>
<u>Wildfire</u>	<u>Any unplanned and uncontrolled vegetation fire that, regardless of ignition source, may negatively affect social, economic or environmental values, and require suppression response or other action according to agency policy (FAO, 2024).</u>	<u>EN0205</u>	<u>FAO (2024)</u>
<u>Runoff Pollution</u>	<u>Nonpoint sources of pollution refer to pollution that does not have a single point of origin or has not been introduced into a receiving freshwater or maritime environment from a specific outlet. The pollutants are generally carried off from the land by agricultural runoff, urban stormwater, atmospheric deposition or subaqueous groundwater discharges. The most common categories of nonpoint pollution are agriculture, forestry, urban areas, mining, construction, dams and channels, land disposal and saltwater intrusion.</u>	<u>EN0106</u>	<u>UNdata (2026) Admad, Sakib and Gang (2016)</u>

Formatted: Font color: Black

Formatted: Normal, Border: Top: (No border), Bottom: (No border), Left: (No border), Right: (No border), Between : (No border), Tab stops: 7.96 cm, Centered + 15.92 cm, Right

<u>Fluvial Flooding</u>	Overflowing by water of the normal confines of a watercourse or other body of water (WMO, 2012).	MH0604	UNESCO and WMO (2012)
<u>*Avulsion Flooding</u>	River avulsions are an abrupt change in a rivers course to establish a new river channel. These are natural phenomena as the river migrates across the floodplain but can result in devastating avulsion floods. Whilst their mechanism is not yet fully understood, they are considered to occur when sediment depositions downstream of the avulsion location cause the existing channel to become unfavourable and so the channel switches to a route with a more efficient flow pathway (Singerland and Smith, 2004; Gearon et al., 2024).	MH0600	Singerland and Smith (2004) Gearon et al. (2024)
<u>River Erosion and Accretion</u>	River erosion is the removal of material from the banks and beds of rivers and streams (Lawler, 1993). River accretion is the formation of new land such as channel bars, sandbanks and deltas by sedimentation or changing river flow (after Islam and Guchhait, 2020 and Hasanuzzaman et al., 2024).	GH0404	Lawler (1993) Hasanuzzaman et al. (2024) Islam and Guchhait (2020)
<u>Debris Flows</u>	Flows are gravitational mass movements down a slope in the form of a fluid. Flows often leave behind a distinctive, fan-shaped deposit where the landslide material has stopped moving (British Geological Survey 2024) Sub-categories of flows may be defined by the type and proportion of material (e.g., soil, debris, or earth and the velocity of the mass movement, Cruden and Varnes, 1996; Hungr, Leroueil and Picarelli, 2014).	GH0303	British Geological Survey (2024) Cruden and Varnes (1996) Hungr, Leroueil and Picarelli (2014)
<u>*Debris Flooding</u>	Debris floods are 'very rapid flow of water, heavily charged with debris, in a steep channel...' in which 'the streambed may be destabilized' (Hungr, Leroueil and Picarelli, 2014) resulting in massive sediment transport over large distances (Church and Jakobs, 2020).	MH0600	Hungr, Leroueil and Picarelli (2014) Church and Jakobs (2020)
<u>Landslide**</u>	A gravitational mass movement ('landslide') is the downslope movement of soil, rock and organic materials under the effects of gravity, which occurs when the gravitational driving forces exceed the frictional resistance of the material resisting on the slope. Such movements may be terrestrial or submarine (GH0306) (Cruden and Varnes, 1996).	GH0300	Cruden and Varnes (1996)

Formatted: Font color: Black

Formatted: Normal, Border: Top: (No border), Bottom: (No border), Left: (No border), Right: (No border), Between : (No border), Tab stops: 7.96 cm, Centered + 15.92 cm, Right

**Here, we define landslides as those connected to the river system.

Heavy Metal Pollution Heavy metals are metallic trace elements with either high relative atomic weights or occurring in materials with high densities. Trace Elements is the term used for elements that are generally found in soil at low concentrations. Trace elements can become contaminants when their concentrations significantly exceed natural levels due to anthropogenic activities, such as industrial processes, mining, agriculture, and waste disposal. These contaminants can accumulate in soil, water, and biota, potentially causing adverse effects on ecosystems and human health.

Table D2: Description of the hazard interactions in Fig. 2 and supporting evidence.

#	Initiating Hazard	Affected Hazard	Interaction Description	Evidence
1	Wildfire	Runoff pollution	Increased probability. Burning of soils and vegetation cover increased their erosion and runoff to the river channel. This hazard is also catalysed by higher rates of erosion increasing the delivery of soil, ash and peat to the river.	Four interview respondents describing increased turbidity immediately after the wildfire and during high flows, with a smell "like methane" [M1, M2, R1, G1].
2	Wildfire	Fluvial flood	Increased probability. Burning of vegetation has reduced interception and root uptake of precipitation, increasing surface runoff to the channel. This has increased peak discharges at reduced lag times following peak rainfall events. The burning and erosion of mature soils has also reduced their infiltration and storage capacities, therefore increasing runoff.	Humanitarian data of 10 flood events since 2012 exceeding the impacts of any documented flood in the 12 years prior (Table 1). Interviewee accounts [M1, M2, G1, G2, R1], e.g. "the burning is the reason we are now having the floods annually... we know how useful wetland vegetation is in controlling floods, releasing water slowly" [G1].
3	Wildfire	River channel erosion	Increased probability. Wildfire's burning of vegetation and erosion of soil has increased runoff, peak river discharge, and therefore the erosive power of the river. Initial erosion and mass movement also exposed river cliffs/riverbanks, which is increasing the probability of (and catalysing) further erosion in a positive feedback process.	GIS analysis calculating an erosion rate increase by a factor of 2.64 due to the wildfire (Fig. 4). Photographs of exposed river cliffs/riverbanks within wildfire affected areas (Fig. 3c and Appendix F).
4	Wildfire	Debris flood	Increased probability. Wildfire has increased peak river discharge by the burning of vegetation and soil which modulate discharge. It has also increased sediment generation through augmented erosion and mass movement, improving the conditions for debris flow/flood development.	Two interview respondents explain and show camera footage of 2013 and 2020 debris flows/floods, described as unprecedented before the fire [M1, R1] (Table 1). Jacob's et al.'s (2016) reconstruction of debris flow/flood during the May 2013 flood. Field photographs of boulder deposition on the delta and distal flood plain (Appendix G).

Formatted: Line spacing: single

Formatted Table

Formatted: Line spacing: single

Formatted: Line spacing: single

Formatted: Font: Times New Roman

Formatted: Line spacing: single

Formatted: Line spacing: single

Formatted: Font color: Black

Formatted: Normal, Border: Top: (No border), Bottom: (No border), Left: (No border), Right: (No border), Between : (No border), Tab stops: 7.96 cm, Centered + 15.92 cm, Right

57	Fluvial flood	Fluvial flood	Increased probability. Fluvial floods damage engineered flood defences, increasing the probability of future breaches.	Photos of damaged flood defences (Appendix H).
68	Fluvial flood	River channel erosion	Triggering. Higher flow velocities and turbulence during fluvial floods exert shear stress, abrasion and hydraulic action to erode river banks riverbanks.	GIS analysis shows the years of highest erosion occurred in 2013 and 2020, the years of the largest debris and fluvial floods [M1, R1] (Fig. 4).
6*	Fluvial flood	Runoff pollution	Triggering. Fluvial floods transport materials across the urban and agricultural landscape. If pollutants are present, this results in a runoff pollution event. *This is also true of avulsion floods and debris floods	Respondents describe post-flood contamination of urban and agricultural landscapes [M1, M2]. Field photographs of contaminant transport into urban areas (Appendix L, Fig. L1).
79	River channel erosion and accretion	Fluvial flood	Increased probability. Eroded material fills and reduces the channel's carrying capacity for discharge. Erosion has also relocated active channels closer to residential areas.	Change in river morphology to a sediment-laden braided system indicating increased deposition and channel switching (Fig. 4b).
810	River channel erosion and accretion	Landslide	Triggering. Lateral and vertical erosion of riverbanks undercuts and destabilises hillslopes, increasing local shear stresses to failure.	Jacobs et al. (2016) map 14 landslides triggered by scour and bank failure from river erosion.
911	River channel erosion and accretion	River channel erosion	Increased probability. Erosion of banks exposes steep, unstable river cliffs riverbanks to further erosion.	Photos of erosional river cliffs riverbanks incising into hillslopes at multiple sites (Appendix F). Interviewee descriptions [G1, G2, M1]
1012	River channel erosion and accretion	Heavy metal pollution	Triggering. River erosion has breached the main 15 Mt solid Co-Cu Kilembe Mines tailings deposit and other smaller deposits within the town.	Satellite images and field photographs (Fig. 4) show erosive river cliffs riverbanks and new channels within the original tailings area. Field observations of downstream deposition of tailings and iron precipitates (Appendix E). Four respondents consider waste deposition a major concern for public health and a potential cause of vegetation death on the riverbanks [M2, W1, G2, R1].
1114	River channel erosion and accretion	Avulsion flood	Triggering. Increased erosion of river banks riverbanks causes channel-switching and subsequent avulsion floods.	Humanitarian data and interview respondents [M1, M2] describing the 22nd May 2024 avulsion flood impacting Kasese town (Table 1).
1213	River channel erosion and accretion	Avulsion flood	Increased probability. Higher rates of upstream erosion increase downstream deposition in channel bars, diverting flow towards river banks riverbanks.	Interview respondents [M1, M2] describing the 22nd May 2024 avulsion flood impacting Kasese town (Table 1) and the increased rate of deposition that has raised dredging and channel clearance costs since the 2012 wildfire [M1, M2, R1].
1317	River channel erosion and accretion	Debris flood	Increased probability. Erosion provides additional sediment that improves the probability of debris flow flow formation.	GIS analysis of increased channel area and width (Fig. 3) filled with coarse sediment in a braided system (Appendix K). Two respondents describe debris flows flows as unprecedented before the fire [M1, R1].

Formatted: Line spacing: single

Formatted: Line spacing: single

Formatted: Line spacing: single

Formatted Table

Formatted: Line spacing: single

Formatted: Line spacing: single

Formatted: Line spacing: single

Formatted: Line spacing: single

Formatted: Line spacing: single

Formatted: Line spacing: single

Formatted: Font color: Black

Formatted: Normal, Border: Top: (No border), Bottom: (No border), Left: (No border), Right: (No border), Between : (No border), Tab stops: 7.96 cm, Centered + 15.92 cm, Right

15	River channel erosion and accretion	River channel erosion	Increased probability. Sediment deposition narrows the active channel cross-section, increasing the flow velocity and erosive potential driving further channel erosion.	Interview respondents describing sediment erosion and accretion processes in river channel [M1, M2, R1, G1, G2]. GIS analysis of increased channel area and width (Fig. 3) filled with coarse sediment in a braided system (Appendix K).
16	River channel erosion and accretion	River channel accretion	Increased probability. Sediment deposition narrows the active channel cross-section, increasing the flow velocity and erosive potential driving further channel erosion (#15). The eroded material replenishes the sediment supply available for sediment deposition (#16), sustaining this cycle.	Interview respondents describing sediment erosion and accretion processes in river channel [M1, M2, R1, G1, G2]. GIS analysis of increased channel area and width (Fig. 3) filled with coarse sediment in a braided system (Appendix K).
14 20	Debris flood	Debris flood	Increased probability. Debris floods damage engineered flood defences, increasing the probability of future breaches.	Photos of damaged flood defences (Appendix H).
15 18	Debris flood	River channel erosion	Triggering. Debris flows have high erosive power (Church & Jakob, 2020); Triggering. Debris floods have high erosive power (Church & Jakob, 2020).	GIS analysis shows the years of highest erosion occurred in 2013 and 2020, the years of the largest debris and fluvial floods [M1, R1] (Appendix K).
19	Debris flood	River channel accretion	Triggering. Debris floods deliver mobilized sediment directly into the river channel, promoting accretion and progressively altering channel geometry over time.	Interview respondents describing the increase in channel sediment deposition following debris flood events [M1; M2; R1].
24	Landslide	Heavy metal pollution	Triggering. Rotational slumping of the soft, unconsolidated tailings into the River Nyamwamba causes heavy metal contamination of water and sediment.	Satellite images and field observations (Appendix K) show rotational slump scars throughout the affected tailings. Four respondents consider waste deposition a major concern for public health and a potential cause of vegetation death on the riverbanks [M2, W1, G2, R1].
23	Landslide	River channel erosion	Increased probability. Landslides increase sediment load and the subsequent erosive power of the river through abrasion.	Interview respondents describing the increase in channel sediment deposition following landslides [R1; M1; M2; I1; G2]. Field photographs of slump scars on riverbanks (Appendix I). Analysis by Jacobs et al. (2016) showing landslides directly entering the river system.
22	Landslide	River channel accretion	Increased probability. Landslides add increase sediment load, accelerating accretion and lateral erosion by diverting flow to the riverbanks.	Interview respondents describing the increase in channel sediment deposition following landslides [R1; M1; M2; I1; G2]. Field photographs of slump scars on riverbanks (Appendix I). Analysis by Jacobs et al. (2016) showing landslides directly entering the river system.

Formatted: Line spacing: single

Formatted Table

Formatted: Line spacing: single

Formatted: Font color: Black

Formatted: Normal, Border: Top: (No border), Bottom: (No border), Left: (No border), Right: (No border), Between : (No border), Tab stops: 7.96 cm, Centered + 15.92 cm, Right

16 21	Landslide	Fluvial flood	<p>Increased probability. Landslide material fills and reduces the channel's carrying capacity for discharge.</p> <p>Landslides also increase the probability of fluvial (and debris) flooding through temporary damming and bursting mechanisms that create surges of discharge.</p>	<p>Jacobs et al. (2016) mapped 29 landslides during the May 2013 flood that directly entered the River Nyamwamba.</p> <p>Five respondents describe a mechanism of temporary landslide damming and bursting "in the space of a few minutes" [M1] during peak rainfall events in the upper-catchment [G1, M1, M2, R1, W1].</p>
17 5	Landslide Runoff pollution	River erosion channel accretion	<p>Increased probability. Landslides increase sediment load and Runoff pollution from the subsequent erosive power burned area transports elevated loads of fine sediment and contaminants into the river through abrasion-channel. Increased sediment supply promotes channel accretion as the excess sediment load settles into the river channel.</p>	<p>Field photographs of slump scars on river banks (Appendix F, Appendix H) Four interview respondents describing increased turbidity immediately after the wildfire and during high flows, with a smell "like methane" [M1, M2, R1, G1].</p> <p>GIS analysis of increased channel area and width (Fig. 3) filled with coarse sediment in a braided system (Appendix K).</p> <p>Analysis by Jacobs et al. (2016) showing landslides directly entering the river system.</p>
18	Landslide	Heavy metal pollution	<p>Triggering. Rotational slumping of the soft, unconsolidated tailings into the River Nyamwamba causes heavy metal contamination of water and sediment.</p>	<p>Satellite images and field observations (Appendix K) show rotational slump scars throughout the affected tailings.</p> <p>Four respondents consider waste deposition a major concern for public health and a potential cause of vegetation death on the riverbanks [M2, W1, G2, R1].</p>

Formatted: Line spacing: single

Formatted Table

Formatted: Line spacing: single

Formatted: Line spacing: single

Formatted: Font color: Black

Formatted: Normal, Border: Top: (No border), Bottom: (No border), Left: (No border), Right: (No border), Between : (No border), Tab stops: 7.96 cm, Centered + 15.92 cm, Right



Formatted: Font color: Black

Formatted: Normal, Border: Top: (No border), Bottom: (No border), Left: (No border), Right: (No border), Between : (No border), Tab stops: 7.96 cm, Centered + 15.92 cm, Right



946
947 **Figure E1: Acid mine drainage at location 0.18599N, 30.01951E, 25 July 2024.**

Formatted: Font color: Black

Formatted: Normal, Border: Top: (No border), Bottom: (No border), Left: (No border), Right: (No border), Between : (No border), Tab stops: 7.96 cm, Centered + 15.92 cm, Right



948

Formatted: Font color: Black

Formatted: Normal, Border: Top: (No border), Bottom: (No border), Left: (No border), Right: (No border), Between : (No border), Tab stops: 7.96 cm, Centered + 15.92 cm, Right



Figure E2: Acid mine drainage at location 0.19879N, 30.01139E, 3 August 2024.

Formatted: Font color: Black

Formatted: Normal, Border: Top: (No border), Bottom: (No border), Left: (No border), Right: (No border), Between : (No border), Tab stops: 7.96 cm, Centered + 15.92 cm, Right



951

44
44

Formatted: Font color: Black

Formatted: Normal, Border: Top: (No border), Bottom: (No border), Left: (No border), Right: (No border), Between : (No border), Tab stops: 7.96 cm, Centered + 15.92 cm, Right



952

45
45

Formatted: Font color: Black

Formatted: Normal, Border: Top: (No border), Bottom: (No border), Left: (No border), Right: (No border), Between : (No border), Tab stops: 7.96 cm, Centered + 15.92 cm, Right

953 Figure E3: Tailings sedimentation in the Nyamwamba channel, 0.18652N, 30.01986E, 25 July 2024.

954 Appendix F: Exposed ~~River Cliffs~~Riverbank Photographs



955

Formatted: Font color: Black

Formatted: Normal, Border: Top: (No border), Bottom: (No border), Left: (No border), Right: (No border), Between : (No border), Tab stops: 7.96 cm, Centered + 15.92 cm, Right



956
957 **Figure F1: River-cliffRiverbank exposure at 0.29291N, 29.93596E – 28 July 2024.**
958

Formatted: Font color: Black

Formatted: Normal, Border: Top: (No border), Bottom: (No border), Left: (No border), Right: (No border), Between : (No border), Tab stops: 7.96 cm, Centered + 15.92 cm, Right



959

48
48

Formatted: Font color: Black

Formatted: Normal, Border: Top: (No border), Bottom: (No border), Left: (No border), Right: (No border), Between : (No border), Tab stops: 7.96 cm, Centered + 15.92 cm, Right



960
961 **Figure F2: River cliff style erosion of house foundations in Kilembe, 0.20603N, 30.00822E – 24 July 2024.**
962
963
964
965
966
967
968
969
970
971

Formatted: Font color: Black

Formatted: Normal, Border: Top: (No border), Bottom: (No border), Left: (No border), Right: (No border), Between : (No border), Tab stops: 7.96 cm, Centered + 15.92 cm, Right

972



973

50
50

Formatted: Font color: Black

Formatted: Normal, Border: Top: (No border), Bottom: (No border), Left: (No border), Right: (No border), Between : (No border), Tab stops: 7.96 cm, Centered + 15.92 cm, Right



974
975 **Figure F3: River cliffRiverbank at 0.23742N, 23.97568E – 1 August 2024.**

Formatted: Font color: Black

Formatted: Normal, Border: Top: (No border), Bottom: (No border), Left: (No border), Right: (No border), Between : (No border), Tab stops: 7.96 cm, Centered + 15.92 cm, Right



976

Formatted: Font color: Black

Formatted: Normal, Border: Top: (No border), Bottom: (No border), Left: (No border), Right: (No border), Between : (No border), Tab stops: 7.96 cm, Centered + 15.92 cm, Right



Figure F4: River cliffRiverbank at 0.23715N, 29.97601E – 1 August 2024.

977
978
979

Formatted: Font color: Black

Formatted: Normal, Border: Top: (No border), Bottom: (No border), Left: (No border), Right: (No border), Between : (No border), Tab stops: 7.96 cm, Centered + 15.92 cm, Right

980 **Appendix G: Flood Plain Boulder Deposition Photographs**



981

54
54

Formatted: Font color: Black

Formatted: Normal, Border: Top: (No border), Bottom: (No border), Left: (No border), Right: (No border), Between : (No border), Tab stops: 7.96 cm, Centered + 15.92 cm, Right



982

983

Figure G1: 0.20285N, 30.00908E - 7 June 2023.

Formatted: Font color: Black

Formatted: Normal, Border: Top: (No border), Bottom: (No border), Left: (No border), Right: (No border), Between : (No border), Tab stops: 7.96 cm, Centered + 15.92 cm, Right



984

Formatted: Font color: Black

Formatted: Normal, Border: Top: (No border), Bottom: (No border), Left: (No border), Right: (No border), Between : (No border), Tab stops: 7.96 cm, Centered + 15.92 cm, Right



985
986 **Figure G2: 0.19528N, 30.01544E - 25 July 2024.**
987

Formatted: Font color: Black

Formatted: Normal, Border: Top: (No border), Bottom: (No border), Left: (No border), Right: (No border), Between : (No border), Tab stops: 7.96 cm, Centered + 15.92 cm, Right

Formatted: Font color: Black

Formatted: Normal, Border: Top: (No border), Bottom: (No border), Left: (No border), Right: (No border), Between : (No border), Tab stops: 7.96 cm, Centered + 15.92 cm, Right



989

Formatted: Font color: Black

Formatted: Normal, Border: Top: (No border), Bottom: (No border), Left: (No border), Right: (No border), Between : (No border), Tab stops: 7.96 cm, Centered + 15.92 cm, Right



Figure H1: 0.18981N, 30.07408E, 26 July 2024 (damaged bamboo nature-based solution).

990
991
992

Formatted: Font color: Black

Formatted: Normal, Border: Top: (No border), Bottom: (No border), Left: (No border), Right: (No border), Between : (No border), Tab stops: 7.96 cm, Centered + 15.92 cm, Right



993

61
61

Formatted: Font color: Black

Formatted: Normal, Border: Top: (No border), Bottom: (No border), Left: (No border), Right: (No border), Between : (No border), Tab stops: 7.96 cm, Centered + 15.92 cm, Right



Formatted: Font color: Black

Formatted: Normal, Border: Top: (No border), Bottom: (No border), Left: (No border), Right: (No border), Between : (No border), Tab stops: 7.96 cm, Centered + 15.92 cm, Right

995 **Figure H2: 0.21387N, 30.00558E, 7 June 2023 (damaged gabions).**

996 **Appendix I: Landslide Talus Entering the River Photographs**



997

Formatted: Font color: Black

Formatted: Normal, Border: Top: (No border), Bottom: (No border), Left: (No border), Right: (No border), Between : (No border), Tab stops: 7.96 cm, Centered + 15.92 cm, Right



998

999

Figure II: 0.29291N, 29.93596E – 28 July 2024.

Formatted: Font color: Black

Formatted: Normal, Border: Top: (No border), Bottom: (No border), Left: (No border), Right: (No border), Between : (No border), Tab stops: 7.96 cm, Centered + 15.92 cm, Right



1000

65
65

Formatted: Font color: Black

Formatted: Normal, Border: Top: (No border), Bottom: (No border), Left: (No border), Right: (No border), Between : (No border), Tab stops: 7.96 cm, Centered + 15.92 cm, Right



Figure I2: Landslide scar at 0.23758N, 29.97570E – 1 August 2024.

Formatted: Font color: Black

Formatted: Normal, Border: Top: (No border), Bottom: (No border), Left: (No border), Right: (No border), Between : (No border), Tab stops: 7.96 cm, Centered + 15.92 cm, Right

1012 **Appendix J: Lower Course Deposition of Solid Mine Tailings Photographs**



1013

Formatted: Font color: Black
Formatted: Normal, Border: Top: (No border), Bottom: (No border), Left: (No border), Right: (No border), Between : (No border), Tab stops: 7.96 cm, Centered + 15.92 cm, Right



Figure J1: Deposition and acid mine drainage downstream of Kilembe Mines 0.19385N, 30.082355 E, 26 July 2024.

Formatted: Font color: Black

Formatted: Normal, Border: Top: (No border), Bottom: (No border), Left: (No border), Right: (No border), Between : (No border), Tab stops: 7.96 cm, Centered + 15.92 cm, Right



Formatted: Font color: Black

Formatted: Normal, Border: Top: (No border), Bottom: (No border), Left: (No border), Right: (No border), Between : (No border), Tab stops: 7.96 cm, Centered + 15.92 cm, Right



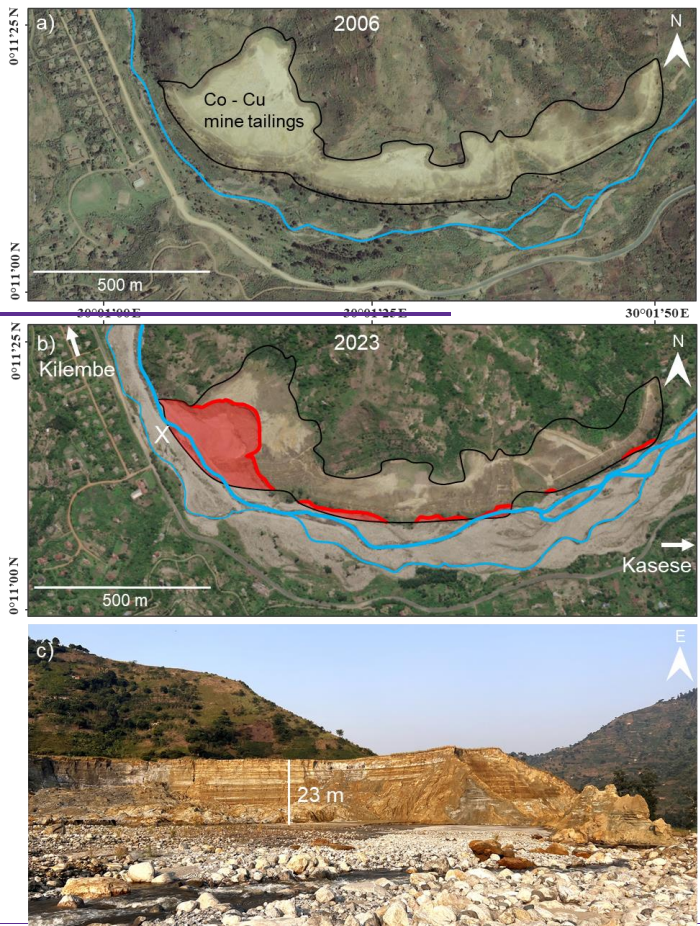
Figure J2: Acid mine drainage from deposited solid tailings at location adjacent to Kasese town, 26 July 2024.

Formatted: Font color: Black

Formatted: Normal, Border: Top: (No border), Bottom: (No border), Left: (No border), Right: (No border), Between : (No border), Tab stops: 7.96 cm, Centered + 15.92 cm, Right

1019 Appendix K: Kilembe Mines Co-Cu Tailings Erosion

1020



Formatted: Font color: Black
Formatted: Normal, Border: Top: (No border), Bottom: (No border), Left: (No border), Right: (No border), Between : (No border), Tab stops: 7.96 cm, Centered + 15.92 cm, Right

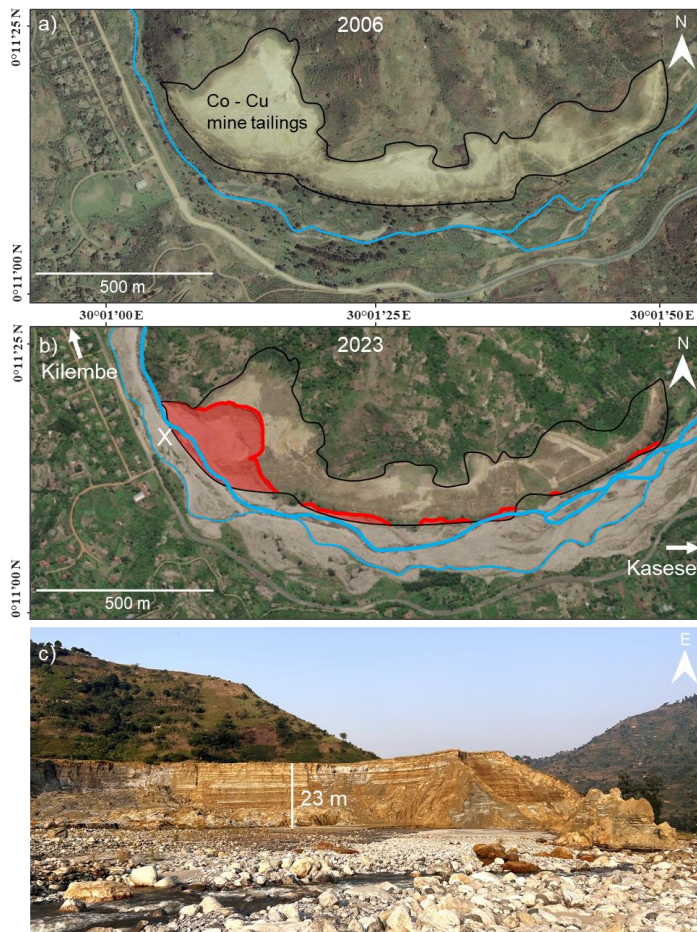


Figure K1 – a) Kilembe Mines tailings on 24th March 2006 (Maxar Technologies, 2024a); b) the same location on 10th Apr 2023 (Maxar Technologies, 2024b) where an estimated 744,000 tonnes of solid waste have eroded into the river. The black polygon outlines the original surface area of mine tailings, and the red polygon shows the area partly or fully eroded; c) photograph of a section of the eroded tailings taken in July 2024 at position X (b), facing east towards Kasese town.

Formatted: Font color: Black

Formatted: Normal, Border: Top: (No border), Bottom: (No border), Left: (No border), Right: (No border), Between : (No border), Tab stops: 7.96 cm, Centered + 15.92 cm, Right

1027 **Appendix L: Post-flood photos from September 2024 flood event**



1028 **Figure L1: Photograph following flooding in Kasese town evidencing the inundation level and post-flood ground**
1029 **contamination. Photograph provided by the Ministry of Water and Environment.**

1031 **Appendix M: Management Strategies and their Evaluation**

1032 The disaster risk management (DRM) strategies in Table L1 have been implemented in the Nyamwamba catchment since the
1033 May 2013 floods. Whilst relocation of communities experiencing near-annual flooding is considered desirable for mitigating
1034 their flood risk [M1, M2, N1], residents have opposed relocation due to existing community and land ties, lower living costs
1035 on flood plain and a lack of economic opportunity in areas proposed for relocation [M1, G2, N1]. Instead, therefore, strategies
1036 have focussed on protecting existing communities and informal settlements on the flood plain with hard engineering,
1037 community-centred and nature-based solutions (Table L1).

1038
1039 **Table L1M1 – Summary of disaster risk reduction strategies in Kasese Districts observed during field reconnaissance and described**
1040 **by interview respondents.**

Formatted: Font color: Black
Formatted: Normal, Border: Top: (No border), Bottom: (No border), Left: (No border), Right: (No border), Between : (No border), Tab stops: 7.96 cm, Centered + 15.92 cm, Right

Strategy	Description	Evaluation	
Hard Engineering	Gabions (Figure L+M1a)	Installed in phases along a 2-3 km alongside Kilembe town to mitigate flooding and river channel switching.	“The Gabions have failed, they’re very weak” [R1]. Damaged by minor flood events (Appendix H), and they have failed to prevent channel overtopping into Kilembe Town during the 22 nd May 2024 flood [M2].
	Channelisation (Figure L+M1b)	A short 500 m channelised section of channel downstream from Kilembe, using concrete to ensure the stability of the road-bridge providing the only access route to Kilembe town.	“what they have done [at the bridge] is perfect...the narrow section never gets clogged up so the rocks pass through” [R1]. The solution has been positively received [R1, R2], but it is considered expensive, and river may switch channels if extended [M2].
	Dredging	5 km of channel is desilted (boulders are broken down and removed from the active water channels to the banks) in an irregular regime, typically funded after major floods such as those in 2013 and 2020 [M1, M2].	It costs US\$4.5 million to clear 5 km of the channel and it needs to be performed annually to maintain a cleared channel [M2]. Residents recall successful desilting by a Canadian mining company until the 1971, so it is a positively viewed activity [G1, G2, W1] but may not be economically sustainable with the currently increased sediment flux of the river [M1]. It does not take place far enough upstream of Kilembe where debris flows/floods generate [R1, M2].
Community-Centred Solutions	Flood Early Warning Systems (Figure L+M1c)	Communities of Kilembe, Kasese and Mubuku given early warnings through the Ugandan Red Cross and the Ugandan Ministry of Water and Environment (MoWE) following alerts of high rainfall.	“with early warning systems, less people are dying... people are more informed with better risk communication” [N1]. However, difficulties monitoring water levels due to high sediment loads and channel switching leaves early warning dependent on rainfall forecasts that are low-confidence in a convectional mountainous region [M2]. Expansion requires greater hydrological monitoring for more accurate, confident and timely warnings [N1, M2].
	Resident Relocation	Relocation of displaced households from Kilembe and river banks riverbanks to the Kasese lowlands, using emergency response funding following major 2013 and 2020 flood events [N1, M1]. Matched with investment to support alternative livelihoods independent of the river such as bee keeping [M1].	In most cases, residents have refused to relocate and are building informal homes [M1]. There is a need for expansion of livelihood incentives and longer-term support investments for their setup [G2]. High flood risk areas offer low-cost land, economic opportunities, free water from the river and many have attachment to lands from family history, mountain livelihoods and lived experience [N1].
	Participatory Desilting	Pilot project training individuals to convert river boulders into crafts, such as granite	It is not being completed at a scale that significantly impacts flood risk [M1], but it has been shown to successfully supplement

Formatted Table

Formatted: Font color: Black
 Formatted: Normal, Border: Top: (No border), Bottom: (No border), Left: (No border), Right: (No border), Between : (No border), Tab stops: 7.96 cm, Centered + 15.92 cm, Right

		wash-basins to be sold to safari lodges and tourists.	family incomes (Ugandan Ministry of Water and Environment (MoWE), 2022);(Ugandan Ministry of Water and Environment (MoWE), 2022). It requires longer-term investment and a plan for expansion and greater access to the market [N1, M1].
Nature-based Solutions (NbS)	River Bank/Riverbank Stabilisation (Figure L4dM1d)	As part of a 2021 World Bank funded project (MoWE, 2022), a 10 km length of the Nyamwamba river-banks/riverbanks have been planted with 30 m thick vegetation buffers to mitigate further lateral erosion. Seedlings planted included 35,000 Asper bamboo, 2,000 mango and 4,000 Mahogany, situated within a fenced zone to deter trespassing, logging, theft and interference by animals (MoWE, 2022).	An existing pilot in Mubuku has demonstrated 20 years of successful bank stabilisation [M1], however 2021 Nyamwamba planting has faced challenges of droughts, floods, termites [W1], death of seedlings due to heavy metal contamination by mine tailings, logging, and reluctant participation by some land owners. Rapid initial growth in patches require long term monitoring and evaluation, but bamboo planting is perceived as the most promising solution for landslide and erosion mitigation in the wildfire-affected zone and around the mine tailings [R1, M1, M2, I1, I2, W1]
	Soil and Water Conservation	Awareness raised among 1,420 land owners of methods available to reduce soil erosion and runoff. 750 were trained to implement the intervention and provided equipment, with 211 hectares of land modified by the addition of trenches and hedges in 2021-2022 (MoWE, 2022). Households encouraged to harvest rainwater instead of drinking from the river.	“there was actually a gentleman that implemented it on his own land, without us telling him to.” Need for more land-owner co-operatives to share trainings, to share risk of failed implementation following land conversion, and to share tedious workloads [G2]. Rainwater harvesting reduces runoff, soil erosion on small plots and decreases heavy metal consumption from river water [M2, G2].
	Afforestation and Regrading of Hillslopes	825 hectares afforested through reforestation and agroforestry in the mid-catchment to reduce landslides, soil erosion and runoff to the river (MoWE, 2022).	Soil-water conservation trenches and soil-stabilising species increased coffee yields [F1]. Some respondents criticised soil-water conservation and afforestation efforts for focussing on the mid-catchment, when “99%” of the sediment and discharge generation is taking place in the burned national park area upstream [R1, I2]. "Until we stabilise those areas [upstream] we will have these problems" [I2].

Formatted Table

1042
1043 For hard engineering strategies, respondents believe that gabions are too weak to sustainably channelise the river [R1, M2]
1044 (Figure L4aM1a), whereas there is demand for the successful concrete channelisation to be extended beyond Kilembe town
1045 centre [R1, R2, M2] (Figure L4bM1b). Channel dredging is perceived to be a critical activity, not because of successful
1046 implementations since 2013, but due to successful historic programmes of dredging by mining companies when Kilembe mines
1047 was operational in the 1960s [G1, G2, W1, R1, M2]. For all hard engineering approaches, there is concern of an unsustainably

Formatted: Font color: Black

Formatted: Normal, Border: Top: (No border), Bottom: (No border), Left: (No border), Right: (No border), Between : (No border), Tab stops: 7.96 cm, Centered + 15.92 cm, Right

1048 high cost of maintenance, given the elevated rate of discharge, erosion and sediment generation in the Nyamwamba river [M1,
1049 M2].

1050
1051 Flood early warning systems piloted in Kilembe and Kasese using 2 local rain gauges and water level sensors have faced
1052 challenges of continuous automated data collection in hard-to-reach upstream locations, however, sharing of information
1053 between authorities and community representatives via Whatsapp has successfully coordinated evacuations following high
1054 flows and rapid dispatches of emergency respondents [N1]. A 2023 installation of a camera 5 km upstream of Kilembe, capable
1055 of international photo and video transmission at 1-minute intervals (Figure 4.14), is considered a useful supplementary
1056 dataset for a more detailed interpretation by those with lived experience and indigenous knowledge of the river [N1, M2]. For
1057 rivers with a debris-flow model of flooding, setting qualitative thresholds of perceived flood severity from imagery may have
1058 more local predictive value than water levels in channels where channel location and roughness change frequently [M2].

1059
1060 A project funded by the World Bank and implemented by the Ugandan Ministry of Water and Environment (MoWE) in 2021
1061 – 2022 has installed a range of nature-based (NbS) and community-centred solutions (MoWE, 2022). The NbS of ~~river~~
1062 ~~bank~~riverbank stabilisation in Kasese is considered especially promising [R1, R3, W1, M1, M2], using 35,000 asper bamboo
1063 seedlings and other economic crops in buffer zones on the mid-catchment ~~river banks~~riverbanks to prevent erosion. Despite
1064 challenges with drought, flooding, termites and metal-contaminated soils during the early implementation [W1, M2, G2], a
1065 previous project successfully stabilising the Mubuku ~~river banks~~riverbanks for 20 years [M1] and observations of stable
1066 bamboo forests in the upper catchment [R1] provide optimism for the project. Respondents are more critical of other parts of
1067 the project, including soil-water conservation and participatory desilting of the river (Table L1), for focussing on the mid-
1068 catchment around Kasese town, when discharge and sediment generation is taking place higher in the mountains [R1, I2].

1069 *“the assumptions made are well off beat; “99% of the water is coming from the park” – R1*

Formatted: Font color: Black

Formatted: Normal, Border: Top: (No border), Bottom: (No border), Left: (No border), Right: (No border), Between : (No border), Tab stops: 7.96 cm, Centered + 15.92 cm, Right



Formatted: Font color: Black

Formatted: Normal, Border: Top: (No border), Bottom: (No border), Left: (No border), Right: (No border), Between : (No border), Tab stops: 7.96 cm, Centered + 15.92 cm, Right



Figure L4MI – Photographs taken during June 2023 field reconnaissance: a) collapsed gabions adjacent to Kilembe town (for scale: 8 m channel width); b) channelisation using concrete embankments in Kilembe town centre (10 m channel width under bridge); c)

Formatted: Font color: Black

Formatted: Normal, Border: Top: (No border), Bottom: (No border), Left: (No border), Right: (No border), Between : (No border), Tab stops: 7.96 cm, Centered + 15.92 cm, Right

1077 **photo from a camera transmitting photos at 1-minute intervals 5 km upstream of Kilembe town centre for flood early warning; d)**
1078 **~~river bank~~riverbank stabilisation adjacent to Kasese town including asper bamboo (4 m fencepost spacing).**

1079 Notably, there have been no DRR interventions so far in the wildfire affected area of the upper catchment, and no active
1080 mitigation of mine tailing erosion into the river Nyamwamba. In both cases, a low awareness of their impacts has inhibited
1081 action [M2, R1, W1, G2]. 7 of 12 interview respondents did not mention the 2012 wildfire when asked to describe factors
1082 affecting local flood risk, and only one small-scale academic study has assessed water quality in the Nyamwamba since large-
1083 scale erosion began in 2015 (~~Mukisa et al., 2020~~)(Mukisa et al., 2020). Of the respondents aware of the wildfire [R1, W1, M1,
1084 M2, G2] and water quality problems [M1, M2, G1, G2] in the Nyamwamba catchment, all recommend restoration of the
1085 wildfire-affected area and urgent mitigation of further erosion into the river.

Formatted: Font color: Black

Formatted: Normal, Border: Top: (No border), Bottom: (No border), Left: (No border), Right: (No border), Between : (No border), Tab stops: 7.96 cm, Centered + 15.92 cm, Right